

Fig. 6. Peroxynitrite induces tyrosine nitration of IRS-1, but not serine phosphorylation of IRS-1. (A) 3T3-L1 adipocytes were incubated with 0, 4 or 8 mM SIN-1 for 12 h, or with 50 ng/ml TNF- α 48 h. The cell lysates were immunoprecipitated with anti-nitrotyrosine or anti-IRS-1 antibody and then immunoblotted with anti-phosphoserine (307)-IRS-1 antibody, anti-insulin receptor β antibody or anti-IRS-1 antibody. (B) 3T3-L1 adipocytes and HIRc were incubated with 0 or 4 mM SIN-1 for 12 h. The cell lysates were used for immunoblotting with anti-IRS-1 antibody. (C) HIRc were incubated with 0, 4 or 8 mM SIN-1 for 12 h, or with 50 ng/ml TNF- α 48 h. The cell lysates were immunoprecipitated with anti-nitrotyrosine or anti-IRS-1 antibody and then immunoblotted with anti-phosphoserine (307)-IRS-1 antibody, anti-insulin receptor β antibody or anti-IRS-1 antibody. This figure shows representative data from three independent experiments.

IRS proteins that act as docking sites for downstream mediators. Among these mediators, PI3-kinase plays an important role in the metabolic actions of insulin and it binds to IRS-1 at its phosphorylated Tyr⁶⁰⁸ and Tyr⁹³⁹ [19]. IRS-1 is also a substrate for various serine kinases, including c-Jun NH₂-terminal kinase [20], Akt [21], inhibitor κ B kinase [8], and protein kinase C [22]. Activation of these kinases by TNF- α or other factors results in impairment of the insulin-signalling pathway and leads to the insulin resistance observed in obesity and type 2 diabetes [23]. In the present study, we investigated the effect of peroxynitrite, which is generated by induction of iNOS, on insulin-stimulated glucose uptake. The importance of iNOS for insulin resistance in vivo is supported by previous studies using iNOS gene-disrupted mice. In these mice, a decrease of IRS-1 phosphorylation by a high-fat diet

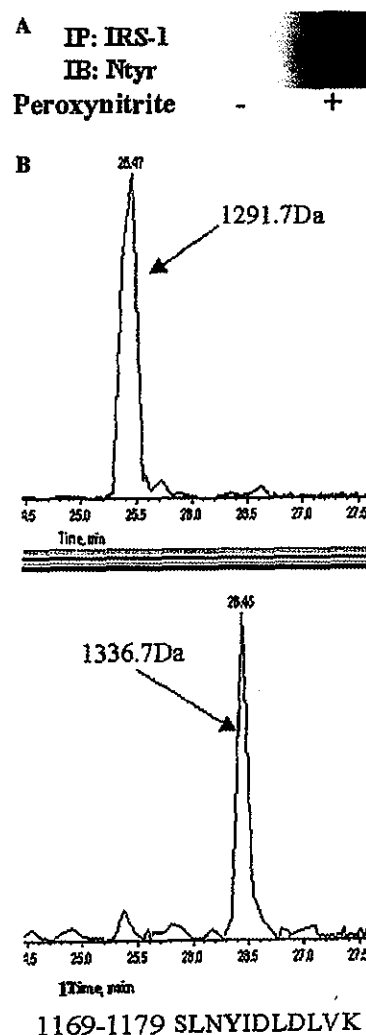


Fig. 7. Identification of nitrated tyrosine residues of rat IRS-1 after exposure to peroxynitrite. (A) One milligram of rat recombinant IRS-1 was incubated with or without 50 μ M peroxynitrite for 1 h at 4 $^{\circ}$ C. Then the sample was immunoprecipitated with anti-IRS-1 antibody and immunoblotted with anti-nitrotyrosine antibody. (B) Representative SIM profiles of peroxynitrite-modified and unmodified peptides. The monitoring ions of both peptides at residues 1169–1179 (SLNY¹¹⁷²IDLVLK) are m/z 646.8 as the $[M+2H]^{2+}$ ion (top) and m/z 669.3 as the $[M+45+2H]^{2+}$ ion (bottom). The molecular weights of the peptides were 1291.7 and 1336.7 Da.

was prevented [10]. Our data showed that peroxynitrite, which is an end-product of iNOS, inhibited insulin-induced glucose uptake, coincident with the tyrosine nitration of IRS-1. Thus, our findings suggested that tyrosine nitration of IRS-1 might also contribute to insulin resistance as does serine phosphorylation of this protein.

We found a decrease of the IRS-1 protein level and IRS-1-mediated signal transduction after treatment with SIN-1. Previous studies have demonstrated that tyrosine-nitrated proteins are more easily degraded [6], thus,

Table 1

Identification of trypsinized peptides of IRS-1 and confirmation of the nitrated tyrosine residues of IRS-1 following treatment with peroxynitrite

Residue	No.	Sequence	Identification of IRS-1		Nitration of Tyr	
			PROWL MS	MASCOT MS/MS	[M + 45 + 2H] ²⁺ SIM	NO ₂ (%) modification
29–33	5	FFVLR	○			
44–51	8	LEYYENEK	○			
82–89	8	HLVALYTR	○	○		
157–166	10	EVWQVILKPK	○	○		
167–172	6	GLGQTK	○			
173–179	7	NLGIYR	○			
192–207	16	LNSEAAAVVLQLMNIR	○	○		
223–253	31	SAVTGPGFEFWMQVDDSVVAQNMHETILEAMR	○			
282–296	15	HHLNPPPSQVGLTR	○			
300–315	16	TESITATSPASMVGGK	○			
316–320	5	PGSFR	○			
489–515	27	YIPGATMGTSALTGDEAAGAADLDNR	○		○	4.1
520–533	14	THSAGTSPTISHQK	○			
534–563	30	TPSQSSVVSIEEYTEMMPAA YPPGGGSGGR	○			
635–647	13	SVSAPQQIINPIR	○	○		
820–838	19	PESSVTHPHHHALQPHLPR	○			
856–862	7	LSLGDPK	○			
871–890	20	EQQQQQQQQSSLHPPEPK	○			
932–948	17	EETGSEEYMNMDLGPGR	○	○	○	26.9
950–962	13	ATWQESGGVELGR	○	○		
976–996	21	PTRSVPNRSDYMTMQIGCPR	○			
997–1014	18	QSYVDTSPVAPVSYADMR	○		○	8.0
1022–1026	5	VSLPR	○			
1027–1073	47	TTGAAPPSSTASASASVTPOGAAEQAAHSSLL GGPQGGGMSAFTR	○			
1169–1179	11	SLNYIDLVLK	○		○	35.3
Total residues (1235)			389	77		
Coverage			31.5%	6.2%		

A mixture of trypsinized peptides was examined by peptide mapping using LC-MS and the PROWL search engine. The amino acid sequences of some peptides were confirmed using LC-MS/MS and the MASCOT search engine. The nitrated tyrosine residues were confirmed by SIM at the [M + 2H]²⁺ and [M + 45 + 2H]²⁺ ions. NO₂ (%) represents the ratio of the ion intensities of the modified and the unmodified tyrosine. Tyrosine residues are shown in bold type.

we speculated that tyrosine-nitrated IRS-1 may also be readily degraded. If so, the reason that we only observed a modest increase of tyrosine nitration of IRS-1 in 3T3-L1 adipocytes treated with SIN-1 (data not shown) might be due to the degradation of IRS-1. In fact, we found a definite increase of tyrosine nitration in HIRC without showing the decrease of the protein level of IRS-1. Thus, tyrosine nitration of IRS-1 may occur by direct modification due to peroxynitrite, and such modification may impair the stability of IRS-1 in a cell-dependent manner.

We used MS to identify the nitrated tyrosine residues in rat IRS-1. The rat IRS-1 protein has 34 tyrosine residues, more than 10 of which can be phosphorylated by insulin receptor tyrosine kinase. In this study, MS covered about 30% of the peptide sequence and showed that at least Tyr⁴⁸⁹, Tyr⁹³⁹, either Tyr⁹⁹⁹ or Tyr¹⁰¹⁰, and Tyr¹¹⁷² residues could be nitrated by peroxynitrite. Among the tyrosine residues of IRS-1, four are found in the src homology 2 (SH2)-binding domain. Among these, Tyr⁶⁰⁸ and Tyr⁹³⁹ are especially considered to be

important tyrosine residues for docking to the p85 subunit of PI3 kinase [6]. Although we could not investigate whether Tyr⁶⁰⁸ was nitrated because of difficulty in isolating a digested peptide including Tyr⁶⁰⁸, nitration of Tyr⁹³⁹ may also inhibit the phosphorylation of IRS-1 at this site and might be involved in the impairment of IRS-1-associated PI3-kinase activity. We showed that treatment with SIN-1 led to the suppression of IRS-1 phosphorylation and more marked suppression of IRS-1-associated p85 activity. These findings suggest that nitration of the tyrosine residues of IRS-1 inhibits tyrosine phosphorylation by the insulin receptor, and thus inhibits its association with p85.

SIN-1 caused more dramatic suppression of IRS-1-associated p85 activity than IRS-1 phosphorylation possibly due to the impairment of PI-3 kinase. Hellberg et al. [24] reported that spermine NONOate, a NO donor, induced tyrosine nitration of the p85 subunit of PI3-kinase in a macrophage cell line. We also detected a modest increase of tyrosine nitration of the p85 subunit together with a modest decrease of the interaction between p85 and

p110. (T.N. and H.W., unpublished observation). Taken together, it is conceivable that various molecules, including p85, are probably involved in the NO-induced reduction of insulin-stimulated glucose uptake. Among these, IRS-1 is certainly the most upstream molecule and one of the most important targets of peroxynitrite in the insulin-signalling cascade (Fig. 4B).

Peroxyntirite is produced by the reaction of NO with superoxide. High blood levels of free fatty acids and glucose, which are often found in diabetes and obesity, can induce the production of superoxide through various mechanisms including increased uptake of substrates by the mitochondria [25]. Thus, once iNOS is induced in insulin-sensitive tissues, peroxyntirite may be easily generated from NO in obese and diabetic individuals. Clinical studies have demonstrated the presence of nitrotyrosine in the blood of diabetic patients, and its level increases in hyperglycaemia [26].

In conclusion, the present study identified a possible mechanism of insulin resistance, which is the main etiological factor of type 2 diabetes and multiple risk factor syndrome. Inhibition of the tyrosine nitration of IRS-1 could be a potentially useful therapeutic target for the treatment of diabetes and related diseases.

Acknowledgments

We thank Dr. J.M. Olefsky for providing HIRc and Drs. K. Egawa, T. Fujita, K. Morino (Shiga University of Medical Science, Otsu, Japan), and F. Yamakura (Juntendo University, Chiba) for the helpful discussion. We also thank Naoko Daimaru for the excellent technical assistance. This work was supported by grants from the Juvenile Diabetes Research Foundation International (to H.W.), the Ministry of Education, Sports and Culture of Japan (to H.U.), and the Takeda Science Foundation (to R.K.).

References

- [1] H.O. Steinberg, G. Brechtel, A. Johnson, N. Fineberg, A.D. Baron, *J. Clin. Invest.* 94 (1994) 1172–1179.
- [2] K.Q. Do, G. Grima, B. Benz, T.E. Salt, *Ann. N. Y. Acad. Sci.* 962 (2002) 81–92.
- [3] C. Nathan, *J. Clin. Invest.* 100 (1997) 2417–2423.
- [4] D.O. Stichtenoht, J.C. Frolich, *Br. J. Rheumatol.* 37 (1998) 246–257.
- [5] R.E. Huie, S. Padmaja, *Free Radic. Res. Commun.* 18 (1993) 195–199.
- [6] A.J. Gow, D. Duran, S. Malcolm, H. Ischiropoulos, *FEBS Lett.* 385 (1996) 63–66.
- [7] X. Li, P. De Sarno, L. Song, J.S. Beckman, R.S. Jope, *Biochem. J.* 331 (Pt. 2) (1998) 599–606.
- [8] Z. Gao, D. Hwang, F. Bataille, M. Lefevre, D. York, M.J. Quon, J. Ye, *J. Biol. Chem.* 277 (2002) 48115–48121.
- [9] S. Kapur, B. Marcotte, A. Marette, *Am. J. Physiol.* 276 (1999) E635–E641.
- [10] M. Perreault, A. Marette, *Nat. Med.* 7 (2001) 1138–1143.
- [11] P.M. Sharma, K. Egawa, T.A. Gustafson, J.L. Martin, J.M. Olefsky, *Mol. Cell. Biol.* 17 (1997) 7386–7397.
- [12] A. Klip, G. Li, W.J. Logan, *Am. J. Physiol.* 247 (1984) E291–E296.
- [13] T. Ogihara, H. Watada, R. Kanno, F. Ikeda, T. Nomiya, Y. Tanaka, A. Nakao, M.S. German, I. Kojima, R. Kawamori, *J. Biol. Chem.* 278 (2003) 21693–21700.
- [14] R. Mineki, H. Taka, T. Fujimura, M. Kikkawa, N. Shindo, K. Murayama, *Proteomics* 2 (2002) 1672–1681.
- [15] U.K. Laemmli, *Nature* 227 (1970) 680–685.
- [16] F. Yamakura, H. Taka, T. Fujimura, K. Murayama, *J. Biol. Chem.* 273 (1998) 14085–14089.
- [17] M.E. Young, G.K. Radda, B. Leighton, *Biochem. J.* 322 (Pt. 1) (1997) 223–228.
- [18] A.R. Saltiel, C.R. Kahn, *Nature* 414 (2001) 799–806.
- [19] X.J. Sun, D.L. Crimmins, M.G. Myers Jr., M. Miralpeix, M.F. White, *Mol. Cell. Biol.* 13 (1993) 7418–7428.
- [20] V. Aguirre, T. Uchida, L. Yenush, R. Davis, M.F. White, *J. Biol. Chem.* 275 (2000) 9047–9054.
- [21] J. Li, K. DeFea, R.A. Roth, *J. Biol. Chem.* 274 (1999) 9351–9356.
- [22] L.V. Ravichandran, D.L. Esposito, J. Chen, M.J. Quon, *J. Biol. Chem.* 276 (2001) 3543–3549.
- [23] S. Mora, J.E. Pessin, *Diabetes Metab. Res. Rev.* 18 (2002) 345–356.
- [24] C.B. Hellberg, S.E. Boggs, E.G. Lapetina, *Biochem. Biophys. Res. Commun.* 252 (1998) 313–317.
- [25] T. Nishikawa, D. Edelstein, X.L. Du, S. Yamagishi, T. Matsumura, Y. Kaneda, M.A. Yorek, D. Beebe, P.J. Oates, H.P. Hammes, I. Giardino, M. Brownlee, *Nature* 404 (2000) 787–790.
- [26] A. Ceriello, F. Mercuri, L. Quagliaro, R. Assaloni, E. Motz, L. Tonutti, C. Taboga, *Diabetologia* 44 (2001) 834–838.



Hypoxia followed by reoxygenation induces secretion of cyclophilin A from cultured rat cardiac myocytes[☆]

Yoshinori Seko,^{a,*} Tsutomu Fujimura,^b Hikari Taka,^b Reiko Mineki,^b Kimie Murayama,^b and Ryozo Nagai^a

^a Department of Cardiovascular Medicine, Graduate School of Medicine, University of Tokyo, Bunkyo-ku, Tokyo, Japan

^b Division of Proteomics and Biomolecular Science, BioMedical Research Center, Graduate School of Medicine, Juntendo University, Bunkyo-ku, Tokyo, Japan

Received 18 February 2004

Abstract

We previously reported that hypoxia followed by reoxygenation (hypoxia/reoxygenation) rapidly activated intracellular signaling such as mitogen-activated protein kinases (MAPKs) including extracellular signal-regulated protein kinase (ERK) 1/2, p38MAPK, and stress-activated protein kinases (SAPKs). To investigate the humoral factors which mediate cardiac response to hypoxia/reoxygenation, we analyzed the conditioned media from cardiac myocytes subjected to hypoxia/reoxygenation by two-dimensional electrophoresis and mass spectrometry. We identified cyclophilin A (CyPA) as one of the proteins secreted from cardiac myocytes in response to hypoxia/reoxygenation. Hypoxia/reoxygenation induced the expression of CyPA and its cell surface receptor CD147 on cardiac myocytes *in vitro*. This was also confirmed by ischemia/reperfusion *in vivo*. Recombinant human (rh) CyPA activated ERK1/2, p38MAPK, SAPKs, and Akt in cultured cardiac myocytes. Furthermore, CyPA significantly increased Bcl-2 in cardiac myocytes. These data strongly suggested that CyPA is released from cardiac myocytes in response to hypoxia/reoxygenation and may protect cardiac myocytes from oxidative stress-induced apoptosis.

© 2004 Elsevier Inc. All rights reserved.

Keywords: Apoptosis; Autocrine; Cardiac myocyte; CD147; Cyclophilin; Hypoxia; Ischemia; Reoxygenation; Reperfusion; Signal transduction

We previously reported that both hypoxia and hypoxia followed by reoxygenation (hypoxia/reoxygenation) rapidly and sequentially activated mitogen-activated protein kinase kinase kinase (MAPKKK) activity of Raf-1, MAP kinase kinase (MAPKK), MAPKs (p44^{Mapk} and p42^{mapk}) (also called extracellular

signal-regulated protein kinase [ERK]1 and ERK2, respectively), and S6 kinase (p90^{rsk}) as well as Src family tyrosine kinases (c-Src and c-Fyn) and p21^{ras}, which are upstream mediators of MAPK pathway [1,2]. We also reported that both hypoxia and hypoxia/reoxygenation rapidly activated stress-activated MAPK signaling cascades involving p65^{PAK}, p38MAPK, and stress-activated protein kinases (SAPKs) in cultured rat cardiac myocytes [3]. Activation of these signaling cascades results in the expression of various genes coding for growth factors, cytokines, cell-adhesion molecules, and so on, which may play a role in the adaptation to these stresses or lead to further cell damage known as reperfusion injury. In this study, to investigate the humoral factors which mediate cardiac response to hypoxia/reoxygenation, we analyzed the conditioned media from cardiac myocytes subjected to hypoxia/reoxygenation and found that cyclophilin A (CyPA) was secreted from cardiac myocytes and might

[☆] **Abbreviations:** BPB, bromophenol blue; CBB, Coomassie brilliant blue; CyPA, cyclophilin A; 2-D, two dimensional; DMEM, Dulbecco's modified Eagle's medium; DTE, dithioerythritol; ERK, extracellular signal-regulated protein kinases; HIV, human immunodeficiency virus; IEF, isoelectric focusing; MAPK, mitogen-activated protein kinase; MAPKK, MAPK kinase; MAPKKK, MAPK kinase kinase; MS, mass spectrometry; PBS, phosphate-buffered saline; PDA, piperazine diacrylamide; SAPK, stress-activated protein kinase; SDS-PAGE, sodium dodecyl sulfate-polyacrylamide gel electrophoresis; Ser, serine; TCA, trichloroacetic acid; TRITC, tetramethyl rhodamine isothiocyanate; TSA, tyramide signal amplification; Tyr, tyrosine; Thr, threonine; VSMC, vascular smooth muscle cell.

* Corresponding author. Fax: +81-3-5689-3815.

E-mail address: sekoyosh-tyk@unin.ac.jp (Y. Seko).

play a role in protecting cardiac myocytes from oxidative stress-induced cell injury.

Materials and methods

Cell culture. Primary cultures of ventricular cardiac myocytes were prepared from neonatal rats as previously described [1]. They were cultured for two days until they were confluent and then serum-starved for 24 h before use.

Hypoxia and reoxygenation. Hypoxic condition (95% N₂, 5% CO₂, and less than 0.1% O₂) was achieved by using an anaerobic jar equipped with a new type AnaeroPack (disposable O₂ absorbing and CO₂ generating agent, Mitsubishi Gas Chemical, Japan) and an indicator to monitor oxygen depletion as described previously [1]. By placing flasks, which contain phosphate-buffered saline (PBS), in an anaerobic jar overnight, the PBS was balanced with the hypoxic atmosphere. Cultured cardiac myocytes were subjected to a hypoxic condition by immediately replacing the medium with the hypoxic PBS in an anaerobic jar. To keep hypoxic conditions, all the procedures were performed in a glove bag filled with 95% N₂ and 5% CO₂. After incubating in a hypoxic condition for 60 min, the cells were reoxygenated by immediately replacing the hypoxic PBS with normoxic PBS for the indicated time periods. We collected the supernatant PBS after 10 min of reoxygenation as reoxygenation-conditioned PBS. We also collected the supernatant PBS after 10 min of incubation with non-stimulated cardiac myocytes under normoxia as control-conditioned PBS.

Two-dimensional gel electrophoresis. We concentrated the reoxygenation-conditioned PBS and control-conditioned PBS by using centrifuge tubes (YM-10; Millipore, Bedford, MA, USA) and collected the fractions of molecular weight >10 kDa from them. Immobilized dry strips at pH 3–10 (7 cm), IPG buffer, PlusOne silver staining kit, and Coomassie brilliant blue (CBB-R350) were purchased from Amersham Biosciences (Uppsala, Sweden). For the first-dimensional isoelectric focusing (IEF), IPGphor strips (7 cm) at pH 3–10 were used. The concentrated-conditioned PBS (50 µg/125 µl) in a microtube (Treff AG, Schweiz, Switzerland) was diluted with Milli Q water (375 µl) and deproteinized with the 500 µl of 40% trichloroacetic acid (TCA) (final concentration 20%). The mixtures were allowed to stand on ice for more than 1 h and centrifuged at 13,000 rpm for 10 min. The supernatants were discarded and the precipitates were washed with cold ether three times to remove excess TCA. The final precipitates were dissolved in the IEF solution containing 9 M urea, 4% CHAPS, 65 mM dithioerythritol (DTE), 2% IPG buffer, pH 3–10, and bromophenol blue (BPB). The dried IPG strips were rehydrated overnight in the sample solution. Then, IEF was performed with the following steps; increasing voltage 30 V for 7 h, 60 V for 7 h, from 60 to 200 V for 0.5 h, from 200 to 500 V for 0.5 h, from 500 to 1000 V for 0.5 h, from 1000 to 8000 V for 0.5 h, and held at 8000 V for 1 h, i.e., a total of 11.5 kV h. Before loading on a 2-D SDS-PAGE, the IPG strips were immersed in 5 ml solution containing 50 mM Tris-HCl (pH 8.5), 6 M urea, 30% glycerol, 2% SDS, 150 mM DTE, and 0.005% BPB and were shaken slowly for 10 min at room temperature in order to reduce the inner and intra-disulfide bonds of cysteinyl residues. And then, the reduced proteins were alkylated with 5 ml of 300 mM acrylamide at room temperature for 10 min. For the 2-D sodium dodecyl sulfate-polyacrylamide gel electrophoresis (SDS-PAGE), we used a gel (110 × 110 × 1 mm; Nihon Eido, Tokyo, Japan), which was prepared for separating gel (10% acrylamide and 2.6% piperazine diacrylamide [PDA]) and for stacking gel (4% acrylamide and 2.6% PDA). The pre-run was performed at 24 mA for 45 min to remove the excess reagents and adjust gel condition. The IPG strips were placed onto the surface of a stacking gel. At first, the 2-D SDS-PAGE commenced at 6 mA for 30 min in order to release proteins from the IPG strips and to stack those into the 2-D gel. Subsequently, the proteins were separated at

12 mA for 3.25 h. The proteins in the gels were stained with the silver staining kit or the CBB R-350 reagent kit and profiled with the image analyzer, Master Scan (Scanalytics, Billerica, MA, USA).

In gel digestion. The proteins on the 2-D SDS-PAGE were subjected to in gel digestion as described previously [4]. The spots were excised manually using a razor blade, placed in microtubes, washed with H₂O (10 min, 37 °C, five times), and destained in 100 µl of 50% CH₃CN and 100 mM ammonium bicarbonate (pH 8.5) for 10 min at 37 °C until colorless. The gels were dehydrated in 100 µl CH₃CN in a microtube for 10 min at 37 °C and was dried in Micro Vac MV-100 (Tomy, Tokyo, Japan) for 5 min. The dried residue was rehydrated by adding 50 µl of 0.001% trypsin in 100 mM ammonium bicarbonate (pH 8.5) and incubated overnight at 37 °C. The incubation mixture in the microtube was centrifuged, and the residue was extracted with 50% CH₃CN and 0.1% trifluoroacetic acid, and centrifuged again. The residue was further extracted with 15% isopropyl alcohol, 20% formic acid, 25% CH₃CN, 40% H₂O, and finally with 80% CH₃CN. The supernatant and all of the extracts were successively dried in a single microtube, and the residue was dissolved in 6 µl of 0.1% formic acid. Aliquots were used for protein identification by mass spectrometry.

Mass spectrometry. Peptide mapping was carried out using API QSTAR Pulsar (I) hybrid mass spectrometer system with a micro-liquid chromatograph (Magic 2002, Michrom BioResource, Auburn, CA, USA). The QSTAR pulsar hybrid mass spectrometer system consists of the apparatus of nanoelectrospray ionization and the quadrupole-time of flight (ESI-TOF) mass spectrometer. Mass accuracy was ±0.1 mass unit. Conditions of mass spectrometry (MS) were as follows; ion spray voltage of 2.0–2.8 kV, voltage for the electron multiplier of 2400 V, nitrogen for curtain gas of 10, nitrogen for collision gas of 10, and collision energy of 20–55 eV for MS/MS analysis. Conditions of micro-LC were as follows; Magic C18 column (0.2 mm, inner diameter × 50 mm) and elution with 0.1% formic acid (solvent A) and 0.1% formic acid in 90% CH₃CN (solvent B) using a program of 3% solvent B for 2 min, gradient at 2.1%/min for 45 min, 100% solvent B for 5 min, and flow rate of 2.5 µl/min. Proteins in-gel digested on 2-D SDS-PAGE were identified with LC-MS/MS using the PROWL (ProFound) and Mascot search engines, and NCBI database.

Ischemia and reperfusion. Rats (male, 250–280 g) were subjected to coronary artery ligation by techniques previously described [5]. Briefly, rats were anesthetized with sodium pentobarbital (40 mg/kg, intraperitoneally), intubated, and ventilated with room air (tidal volume, 20 ml/kg at rate of 60/min) with a respirator (SN-480-7, Shinano Manufacturing, Tokyo, Japan). After lateral thoracotomy and pericardiectomy, a 6–0 silk suture was placed near the intramyocardial location of the left coronary artery beneath the left atrial appendage. We performed coronary artery occlusion by pressing a short length of tube over the ends of the suture and clamping it firmly against the heart. We achieved reperfusion by removing the clamp. The standard limb lead II electrocardiogram was monitored continuously. We confirmed the ischemia and reperfusion of the regional myocardium by following the changes of the ST segment level on the electrocardiogram and observing the change in the color of the myocardium.

Immunohistochemistry. We used tyramide signal amplification (TSA) technology for fluorescence (TSA-Direct [Green], NEN Life Science Products, according to the manufacturer's instructions). Rats were killed at each time point after myocardial ischemia/reperfusion. Cryostat sections (6-µm thick) of heart ventricles were prepared, air-dried, and fixed in acetone for 5 min. After washing in PBS, the sections were incubated with rabbit polyclonal anti-CyPA antibody (Upstate Biotechnology, NY, USA) or goat polyclonal anti-CD147 antibody (G-19; Santa Cruz Biotechnology, CA, USA) for 1 h at 37 °C. After washing in PBS, the sections were incubated with biotinylated anti-rabbit or goat IgG antibody (Vector Laboratories, CA) for 1 h at 37 °C. After washing in TNT buffer (0.1 mol/L Tris-HCl, pH 7.5,

0.15 mol/L NaCl, and 0.05% Tween 20), the sections were blocked with TNB buffer containing a blocking reagent for 30 min and then incubated with streptavidin–horseradish peroxidase for 30 min. After washing in TNT buffer, the sections were incubated with fluorescein–tyramide for appropriate time (3–10 min), washed in TNT buffer, and then examined, and photographed under a fluorescence microscope.

Immunocytochemistry. For immunocytochemical analysis, to distinguish cardiac myocytes from non-muscle cells (mainly consisted of fibroblasts), we performed double-staining for cardiac myosin and CyPA or CD147 using a mouse anti-cardiac myosin monoclonal antibody (mAb) (CMA19) [6] and tetramethyl rhodamine isothiocyanate (TRITC)-conjugated anti-mouse IgG antibody as described previously [7]. The procedures for staining of CyPA and CD147 were the same as for the tissue samples.

Western blot analyses for phosphorylation of ERK1/2, p38MAPK, SAPKs, and Akt. Cardiac myocytes were treated with 10 nM of recombinant human (rh) CyPA (Sigma Chemical, MO, USA) for the indicated time periods, then the culture media were aspirated immediately and cardiac myocytes were frozen in liquid nitrogen. The cells were lysed on ice with buffer A and the cell lysates were centrifuged, as described previously [3]. The supernatants were suspended in Laemmli's sample buffer. Aliquots of the samples were subjected to Western blot analyses using a rabbit polyclonal phospho-specific anti-ERK1/2 (Thr202/Tyr204), p38MAPK (Tyr182), SAPKs (Thr183/Tyr185), or Akt (Ser473) antibody (New England Biolabs, MA, USA), respectively. Aliquots of the same samples were also subjected to Western blot analyses using a rabbit polyclonal control anti-ERK1/2, p38MAPK, SAPKs, or Akt antibody (New England Biolabs), respectively. The antibody–antigen complexes were developed with chemiluminescence using alkaline phosphatase (New England Biolabs).

Western blot analyses for Bcl-2 and Bcl-X. Cardiac myocytes were treated with 50 nM rhCyPA for the indicated time periods. The procedures for preparing the Western blot samples were the same as described above. Aliquots of the samples were subjected to Western blot analyses using mouse anti-Bcl-2 or -Bcl-X mAb (Transduction Laboratories, Lexington, KY, USA). Aliquots of the same samples were subjected to Western blot analysis using a goat polyclonal anti-actin (I-19) antibody (Santa Cruz Biotechnology). The antibody–antigen complexes were developed with chemiluminescence using alkaline phosphatase.

Results

Cultured cardiac myocytes secrete CyPA in response to hypoxia/reoxygenation

Fig. 1 shows the results of 2-D gel electrophoresis of control conditioned PBS (panel A) and reoxygenation-conditioned PBS (panel B) stained with silver. A protein spot (M_r 18.2 kDa and pI 8.4) indicated by an arrow (panel B) was not present in control-conditioned PBS (panel A) and seemed to appear in response to hypoxia/reoxygenation. LC-MS/MS analysis of the protein spot identified CyPA.

Hypoxia/reoxygenation induces expression of CyPA and CD147 on cultured cardiac myocytes in vitro

Next, we examined whether cardiac myocytes express CyPA and its cell surface receptor CD147 under normal condition and in response to hypoxia/reoxygenation. Fig. 2 shows double-stained cultured cardiac myocytes under normal condition or subjected to hypoxia/reoxygenation. Panels A, B, and E show the staining pattern specific for CyPA. Panel F shows the staining pattern specific for CD147. Panels C, D, G, and H which correspond to panels A, B, E, and F, respectively, show the staining pattern specific for cardiac myosin heavy chain and indicate that most of the cells were cardiac myocytes. There was only weak expression of CyPA on cardiac myocytes under normal condition (panel A). No significant change in the expression of CyPA was seen on cardiac myocytes subjected to hypoxia for 60 min (panel B). Most of the cardiac myocytes subjected to hypoxia for 60 min followed by reoxygenation for 10 min moderately to strongly expressed CyPA on their

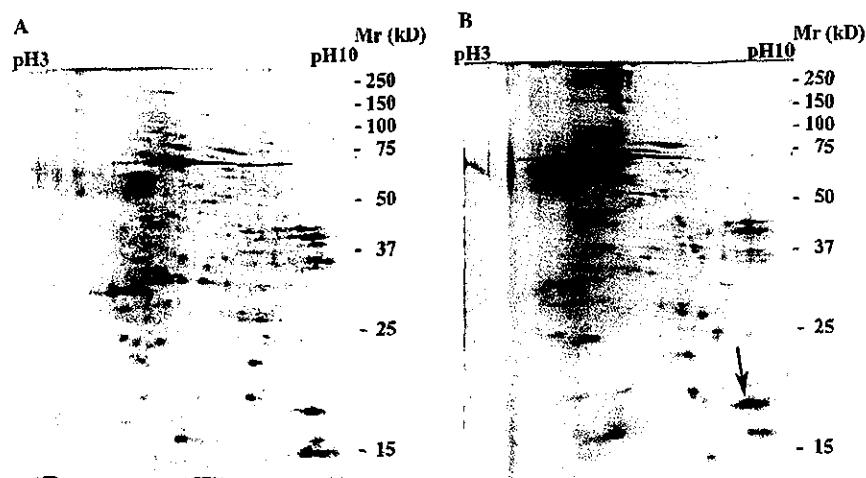


Fig. 1. 2-D gel electrophoresis of control-conditioned PBS (A) and reoxygenation-conditioned PBS (B) stained with silver. An arrow indicates a protein spot (B), which is not present in control-PBS (A).

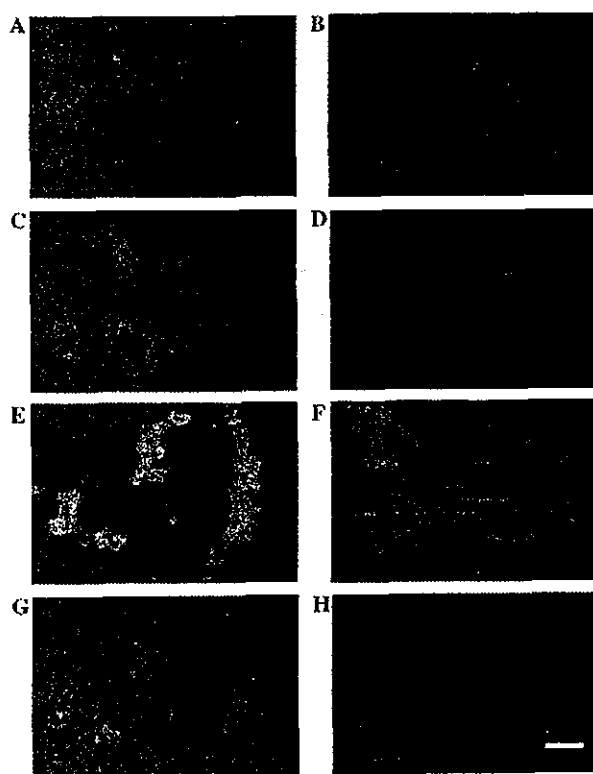


Fig. 2. Immunocytochemical study of cultured cardiac myocytes for CyPA and CD147. (A, B, E, and F) Myocytes under normal condition (A), myocytes subjected to hypoxia for 60 min (B), and myocytes subjected to hypoxia for 60 min followed by reoxygenation for 10 min (E), stained with anti-CyPA antibody, and labeled with FITC. Myocytes under normal condition (F) stained with anti-CD147 antibody and labeled with FITC. Panels C, D, G, and H which correspond to panels A, B, E, and F, respectively, show the staining pattern specific for cardiac myosin heavy chain and labeled with TRITC. Bar = 50 μ m.

surfaces (panel E). Strong expression of CD147 was seen on cardiac myocytes under normal condition (panel F). The expression levels of CD147 on cardiac myocytes

were not significantly changed by hypoxia or by hypoxia/reoxygenation in vitro (data not shown).

Ischemia/reperfusion induces expression of CyPA and CD147 on cardiac myocytes in vivo

To confirm the expression of CyPA and CD147 on cardiac myocytes in vivo, we examined their expression in ventricular tissues from sham-operated rats and rats subjected to myocardial ischemia/reperfusion. In sham-operated rats and rats subjected to myocardial ischemia for 30 min, there was only weak or almost no expression of CyPA on cardiac myocytes (Figs. 3A and B, respectively). In rats subjected to myocardial ischemia for 30 min followed by reperfusion for 15 min, there was a clear expression of CyPA on most of the cardiac myocytes (Fig. 3C). In sham-operated rats and rats subjected to myocardial ischemia for 30 min, there was a moderate expression of CD147 on most of the cardiac myocytes (Figs. 3D and E, respectively). Myocardial ischemia for 30 min followed by reperfusion for 30 min significantly increased the expression of CD147 on most of the cardiac myocytes (Fig. 3F).

CyPA activates ERK1/2, p38MAPK, SAPKs, and Akt in cultured cardiac myocytes

To investigate whether CyPA transduces signals through CD147 and stimulates cardiac myocytes, we examined whether rhCyPA phosphorylates MAPK family members ERK1/2, p38MAPK, and SAPKs, as well as Akt in cultured cardiac myocytes. As shown in Figs. 4A, B, and C, rhCyPA significantly phosphorylated ERK1/2, p38MAPK, and SAPKs, indicating the activation of these kinases. The phosphorylation was led to a maximum level biphasically at 2–5 min and 30 min for ERK1/2 and SAPKs, and at 5–10 min and 30 min for p38MAPK. rhCyPA also significantly phosphorylated

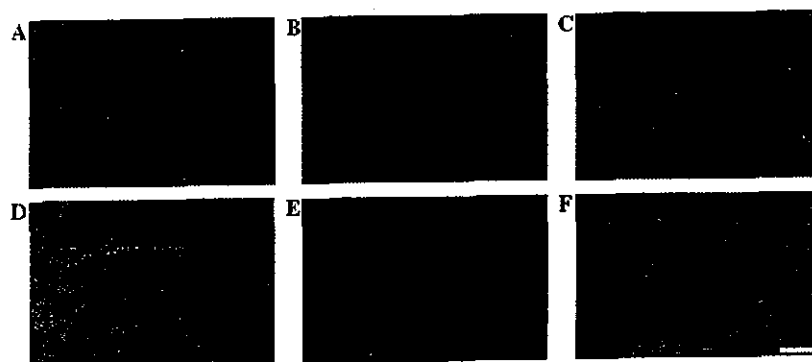


Fig. 3. Immunohistochemical study of ventricular myocardium for CyPA and CD147. Sham-operated myocardium (A), myocardium subjected to ischemia for 30 min (B), and myocardium subjected to ischemia for 30 min followed by reperfusion for 15 min (C) were stained with anti-CyPA antibody. Sham-operated myocardium (D), myocardium subjected to ischemia for 30 min (E), and myocardium subjected to ischemia for 30 min followed by reperfusion for 30 min (F) were stained with anti-CD147 antibody. Bar = 50 μ m.

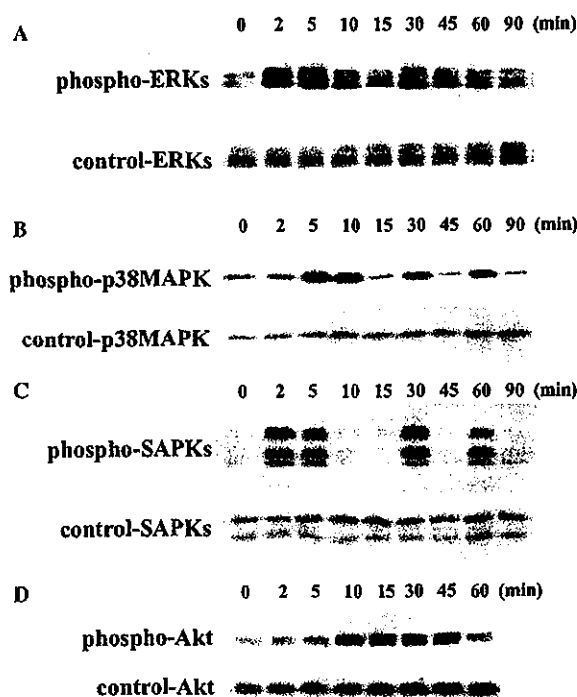


Fig. 4. Recombinant human (rh) CyPA phosphorylates ERK1/2, p38MAPK, SAPKs, and Akt. Serum-starved cardiac myocytes were treated with recombinant human (rh) CyPA (10 nM) for the indicated time periods and lysed in buffer A. The cell lysates were centrifuged and the supernatants were subjected to Western blot analyses using a phospho-specific ERK1/2 (Thr202/Tyr204) (A), p38MAPK (Tyr182) (B), SAPKs (Thr183/Tyr185) (C), or Akt (Ser473) (D) antibody, respectively. Aliquots of the same samples were also subjected to Western blot analyses using a rabbit polyclonal control anti-ERK1/2 (A), p38MAPK (B), SAPK (C), or Akt (D) antibody. The antibody-antigen complexes were developed with chemiluminescence using alkalinephosphatase. The experiments were performed at least in triplicate. The results shown are from one typical experiment.

Akt with a maximum level at 15–30 min. We confirmed that almost equal amounts of ERK1/2, p38MAPK, SAPKs, and Akt proteins were electrophoresed in each reaction by Western blot analyses using control anti-ERK1/2, -p38MAPK, -SAPKs, and -Akt antibodies (phosphorylation-state independent) (Fig. 4).

CyPA increases the expression of Bcl-2 in cultured cardiac myocytes

Because CyPA activates Akt in cardiac myocytes, next, we examined whether CyPA increases anti-apoptotic proteins such as Bcl-2 and Bcl-X_L in cardiac myocytes. As shown in Fig. 5, CyPA significantly increased Bcl-2 with a maximum level at 16 h, whereas CyPA did not significantly change the levels of Bcl-X_L and Bcl-X_S. Western blot analysis using an anti-actin antibody as an internal standard showed that almost equal amounts of samples were electrophoresed in each reaction (Fig. 5).

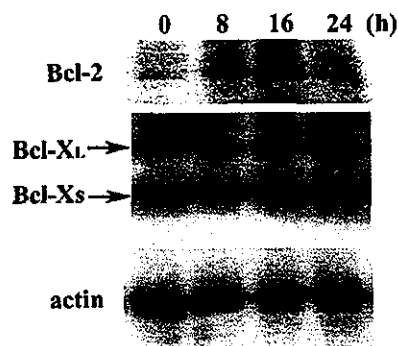


Fig. 5. Effects of recombinant human (rh) CyPA on the expression of Bcl-2 and Bcl-X_{S/L}. Serum-starved cardiac myocytes were treated with rhCyPA (50 nM) for the indicated time periods and lysed in buffer A. The cell lysates were centrifuged and the supernatants were subjected to Western blot analyses using an anti-Bcl-2 or -Bcl-X mAb. Aliquots of the same samples were also subjected to Western blot analysis using an anti-actin antibody. The antibody-antigen complexes were developed with chemiluminescence using alkalinephosphatase. The experiments were performed at least in triplicate. The results shown are from one typical experiment.

Discussion

In the present study, we have showed that CyPA was one of the proteins secreted from cultured rat cardiac myocytes in response to hypoxia/reoxygenation and that hypoxia/reoxygenation induced the expression of CyPA and its cell surface receptor CD147 [8] on cardiac myocytes. This strongly suggests that secreted CyPA interacts with CD147 on cardiac myocytes in an autocrine fashion and plays a role in activating intracellular signaling which mediates cardiac response to hypoxia/reoxygenation. We also showed that rhCyPA activated MAPK family kinases and Akt, and significantly increased Bcl-2 in cardiac myocytes, suggesting a protective role for CyPA against oxidative stress-induced apoptosis.

CyPA is an immunophilin family protein known to exist intracellularly and is distributed ubiquitously. CyPA is known to be an enzyme with peptidyl-prolyl *cis-trans* isomerase activity and acts as a molecular chaperone in protein folding [9,10]. In fact, CyPA has been shown to bind with cyclosporine A or is incorporated into human immunodeficiency virus type 1 (HIV-1) particles, and plays an essential role in immunosuppressive effect of cyclosporine A as well as HIV-1 infection [11–13]. In addition to the intracellular function, CyPA has also been shown to be secreted by cells in response to various stimuli and play important roles in chemotaxis of neutrophils, monocytes, and eosinophils as well as in protecting host cells from external stresses [14–16]. Jin et al. [16] reported that CyPA was secreted by vascular smooth muscle cells (VSMCs) in response to oxidative stress induced by LY83583, an O₂⁻ generator, and that secreted CyPA-mediated ERK activation in VSMCs, increased DNA synthesis, and

inhibited nitric oxide-induced apoptosis in VSMCs. The authors also demonstrated that the expression of CyPA was markedly increased in the balloon-injured vascular lesion, suggesting that CyPA acts as an oxidative stress-responsive growth and survival factor for VSMCs. It has been shown that mammalian cells quickly respond and adapt to external stresses such as mechanical load, metabolic changes, and hypoxia/reoxygenation, by expressing a number of various genes, which may have protective or injurious effects on the cells. In particular, cardiac myocytes express various genes coding for growth factors, cytokines, cell-adhesion molecules, and so on, in response to ischemia/reperfusion to adapt to these stresses or lead to further cell damage known as reperfusion injury. Moreover, evidence has accumulated that cardiac myocytes secrete various growth factors such as angiotensin II, transforming growth factor- β 1, endothelin-1, atrial natriuretic peptide, and adrenomedullin, which in turn mediate cellular response to external stresses in an autocrine fashion [17–21]. Kitta et al. [22] reported that hepatocyte growth factor protected cardiac myocytes against apoptosis induced by oxidative stresses such as daunorubicin, serum deprivation, and hydrogen peroxide. In the present study, we have demonstrated for the first time that cardiac myocytes secreted CyPA in response to hypoxia/reoxygenation and that secreted CyPA played a role in activating intracellular signaling through CD147, which was upregulated on cardiac myocytes by hypoxia/reoxygenation. Upregulation of CyPA and CD147 on cardiac myocytes was also confirmed by ischemia/reperfusion in vivo, suggesting that the similar mechanism was involved in cardiac response to ischemia/reperfusion in vivo. Although at least several growth factors may be involved in the cardiac response to oxidative stresses, our data strongly suggest that CyPA plays a role in the protection of cardiac myocytes against oxidative stress-induced apoptosis through this autocrine mechanism.

Acknowledgments

This work was supported by a grant for scientific research from the Ministry of Education, Culture, Sports, Science and Technology, Japan. We thank Mr. S. Kawano, Mr. T. Shino, and Ms. M. Otsuki for their excellent technical assistance.

References

- [1] Y. Seko, K. Tobe, K. Ueki, T. Kadowaki, Y. Yazaki, Hypoxia and hypoxia/reoxygenation activate Raf-1, mitogen-activated protein (MAP) kinase kinase, MAP kinases, and S6 kinase in cultured rat cardiac myocytes, *Circ. Res.* 78 (1996) 82–90.
- [2] Y. Seko, K. Tobe, N. Takahashi, Y. Kaburagi, T. Kadowaki, Y. Yazaki, Hypoxia and hypoxia/reoxygenation activate src family tyrosine kinases and p21^{ras} in cultured rat cardiac myocytes, *Biochem. Biophys. Res. Commun.* 226 (1996) 530–535.
- [3] Y. Seko, N. Takahashi, K. Tobe, T. Kadowaki, Y. Yazaki, Hypoxia and hypoxia/reoxygenation activate p65^{PAK}, p38 mitogen-activated protein kinase (MAPK), and stress-activated protein kinase (SAPK) in cultured rat cardiac myocytes, *Biochem. Biophys. Res. Commun.* 239 (1997) 840–844.
- [4] R. Mineki, H. Taka, T. Fujimura, M. Kikkawa, N. Shindo, K. Murayama, In situ alkylation with acrylamide for identification of cysteinyl residues in proteins during one- and two-dimensional sodium dodecyl sulphate-polyacrylamide gel electrophoresis, *Proteomics* 2 (2002) 1672–1681.
- [5] H. Selye, E. Bajusz, S. Grasso, P. Mendell, Simple techniques for the surgical occlusion of coronary vessels in the rat, *Angiology* 11 (1960) 398–407.
- [6] Y. Yazaki, H. Tsuchimochi, M. Kuro-o, M. Kurabayashi, M. Isobe, S. Ueda, R. Nagai, F. Takaku, Distribution of myosin isozymes in human atrial and ventricular myocardium: comparison in normal and overloaded heart, *Eur. Heart J.* 5 (Suppl. F) (1984) 103–110.
- [7] Y. Seko, N. Takahashi, M. Azuma, H. Yagita, K. Okumura, Y. Yazaki, Effects of in vivo administration of anti-B7-1/B7-2 monoclonal antibodies on murine acute myocarditis caused by coxsackievirus B3, *Circ. Res.* 82 (1998) 613–618.
- [8] V. Yurchenko, G. Zybarth, M. O'Connor, W.W. Dai, G. Franchin, T. Hao, H. Guo, H.-C. Hung, B. Toole, P. Gallay, B. Sherry, M. Bukrinsky, Active site residues of cyclophilin A are crucial for its signaling activity via CD147, *J. Biol. Chem.* 277 (2002) 22959–22965.
- [9] A. Galat, Peptidylproline *cis-trans*-isomerases: immunophilins, *Eur. J. Biochem.* 216 (1993) 689–707.
- [10] S.F. Gothel, M.A. Marahiel, Peptidyl-prolyl *cis-trans* isomerases, a superfamily of ubiquitous folding catalysts, *Cell Mol. Life Sci.* 55 (1999) 423–436.
- [11] J. Liu, FK506 and cyclosporine, molecular probes for studying intracellular signal transduction, *Immunol. Today* 14 (1993) 290–295.
- [12] D.A. Fruman, S.J. Burakoff, B.E. Bierer, Immunophilins in protein folding and immunosuppression, *FASEB J.* 8 (1994) 391–400.
- [13] J. Luban, K.L. Bossolt, E.K. Franke, G.V. Kalpana, S.P. Goff, Human immunodeficiency virus type 1 Gag protein binds to cyclophilins A and B, *Cell* 73 (1993) 1067–1078.
- [14] B. Sherry, N. Yarlett, A. Strupp, A. Cerami, Identification of cyclophilin as a proinflammatory secretory product of lipopolysaccharide-activated macrophages, *Proc. Natl. Acad. Sci. USA* 89 (1992) 3511–3515.
- [15] Q. Xu, M.C. Leiva, S.A. Fischkoff, R.E. Handschumacher, C.R. Lytle, Leukocyte chemotactic activity of cyclophilin, *J. Biol. Chem.* 267 (1992) 11968–11971.
- [16] Z.-G. Jin, M.G. Melaragno, D.-F. Liao, C. Yan, J. Haendeler, Y.-A. Suh, J.D. Lambeth, B.C. Berk, Cyclophilin A is a secreted growth factor induced by oxidative stress, *Circ. Res.* 87 (2000) 789–796.
- [17] J. Sadoshima, Y. Xu, H.S. Slayter, S. Izumo, Autocrine release of angiotensin II mediates stretch-induced hypertrophy of cardiac myocytes in vitro, *Cell* 75 (1993) 977–984.
- [18] N. Takahashi, A. Calderone, N.J. Izzo Jr., T.M. Maki, J.D. Marsh, W.S. Colucci, Hypertrophic stimuli induce transforming growth factor-beta 1 expression in rat ventricular myocytes, *J. Clin. Invest.* 94 (1994) 1470–1476.
- [19] Y. Bezie, L. Mesnard, D. Longrois, F. Samson, C. Perret, J.J. Mercadier, S. Laurent, Interactions between endothelin-1 and atrial natriuretic peptide influence cultured chick cardiac myocyte contractility, *Eur. J. Pharmacol.* 311 (1996) 241–248.
- [20] T. Horio, T. Nishikimi, F. Yoshihara, H. Matsuo, S. Takishita, K. Kangawa, Inhibitory regulation of hypertrophy by endogenous atrial natriuretic peptide in cultured cardiac myocytes, *Hypertension* 35 (2000) 19–24.

- [21] F. Yoshihara, T. Horio, T. Nishikimi, H. Matsuo, S. Kangawa, Possible involvement of oxidative stress in hypoxia-induced adrenomedullin secretion in cultured rat cardiomyocytes, *Eur. J. Pharmacol.* 436 (2002) 1–6.
- [22] K. Kitta, R.M. Day, T. Ikeda, Y.J. Suzuki, Hepatocyte growth factor protects cardiac myocytes against oxidative stress-induced apoptosis, *Free Radic. Biol. Med.* 31 (2001) 902–910.

Membrane-Associated IL-1 Contributes to Chronic Synovitis and Cartilage Destruction in Human IL-1 α Transgenic Mice

Yasuo Niki,^{1,2,*} Harumoto Yamada,[†] Toshiyuki Kikuchi,[‡] Yoshiaki Toyama,^{*} Hideo Matsumoto,^{*} Kyosuke Fujikawa,[‡] and Norihiro Tada[§]

IL-1 molecules are encoded by two distinct genes, IL-1 α and IL-1 β . Both isoforms possess essentially identical activities and potencies, whereas IL-1 α , in contrast to IL-1 β , is known to act as a membrane-associated IL-1 (MA-IL-1) and plays an important role in a variety of inflammatory situations. The transgenic (Tg) mouse line (Tg1706), which was generated in our laboratory, overexpresses human IL-1 α (hIL-1 α) and exhibits a severe arthritic phenotype characterized by autonomous synovial proliferation with subsequent cartilage destruction. Because the transgene encoded Lys⁶⁴ to Ala²⁷¹ of the hIL-1 α amino acid sequence, Tg mice may overproduce MA-IL-1 as well as soluble IL-1 α . The present study investigated whether MA-IL-1 contributes to synovial proliferation and cartilage destruction in the development of arthritis. Flow cytometric analysis revealed that both macrophage-like and fibroblast-like synoviocytes constitutively produce MA-IL-1. D10 cell proliferation assay revealed MA-IL-1 bioactivity of paraformaldehyde-fixed synoviocytes and the further induction of endogenous mouse MA-IL-1 via autocrine mechanisms. MA-IL-1 expressed on synoviocytes triggered synoviocyte self-proliferation through cell-to-cell (i.e., juxtacrine) interactions and also promoted proteoglycan release from the cartilage matrix in chondrocyte monolayer culture. Interestingly, the severity of arthritis was significantly correlated with MA-IL-1 activity rather than with soluble IL-1 α activity or concentration of serum hIL-1 α . Moreover, when the Tg1706 line was compared with the Tg101 line, which selectively overexpresses the 17-kDa mature hIL-1 α , the severity of arthritis was significantly higher in the Tg1706 line than in the Tg101 line. These results suggest that MA-IL-1 contributes to synoviocyte self-proliferation and subsequent cartilage destruction in inflammatory joint disease such as rheumatoid arthritis. *The Journal of Immunology*, 2004, 172: 577–584.

Rheumatoid arthritis (RA)³ is characterized by a permanently proliferative synovium, leading to the formation of hyperplastic synovial tissue (pannus) that invades both cartilage and bone. Human IL-1 α (hIL-1 α) transgenic (Tg) mice overexpressing hIL-1 α exhibit macrophage- and neutrophil-dominant arthritis characterized by marked synovial proliferation and progressive cartilage destruction, resembling RA with a progressive phenotype. Histopathological analysis of synovial joints from hIL-1 α Tg mice has demonstrated that proliferative synovium directly invades the cartilage, ultimately destroying both cartilage and underlying bone (1). As IL-1 is known to play a pivotal role in the pathogenesis of RA, analysis of IL-1-mediated synovial proliferation and subsequent invasion of the cartilage may elucidate the mechanisms of joint destruction and suggest new therapies for RA.

IL-1 molecules are encoded by two distinct genes, IL-1 α and IL-1 β . Both genes initially produce precursor polypeptides with a predicted M_r of 31 kDa. IL-1 α precursor is fully biologically active and acts as a membrane-associated IL-1 (MA-IL-1), whereas

IL-1 β precursor displays no biological activity until it has been processed to form the 17-kDa mature form (2, 3). Unlike other secreted proteins, IL-1 α precursor lacks a hydrophobic leader sequence (4) and is never found in organelles involved in the classical secretory pathway. The processing and release of IL-1 α demonstrate atypical regulation through a number of post-translational modifications (5–7), and the exact processes vary between different cell types (8–10). Our detailed analysis of hIL-1 α Tg mice revealed that among various cell types, synoviocytes are the predominant cells producing both precursor and processed forms of hIL-1 α despite the use of ubiquitous CAG promoter. This preferential distribution of hIL-1 α in synoviocytes seems at least partially due to the extended retention of MA-IL-1 in these cells (1).

In certain situations, IL-1 α reportedly acts preferentially as MA-IL-1 (11), which was first described as IL-1 bioactivity within paraformaldehyde (PFA)-fixed macrophage or purified macrophage membranes (12). The presence of IL-1 α has subsequently been demonstrated on the surface of various cell types (13–19). A wide spectrum of biological properties has also been reported, including induction of autonomous proliferation in vascular smooth muscle cells (20), T cell activation during Ag presentation (21), up-regulation of monocyte/macrophage-mediated tumor cytotoxicity (22), and stimulation of osteoclast formation (23), where cell-to-cell (i.e., juxtacrine) interactions play a key role in these actions.

The hIL-1 α Tg mouse line established in our laboratory was designed to integrate a 660-bp *HindIII/HincII* restriction fragment of hIL-1 α cDNA coding Lys⁶⁴ to Ala²⁷¹ of the hIL-1 α amino acid sequence in an attempt to overproduce both pro and mature forms of IL-1 α . As the transgene includes a nuclear localization sequence (aa 79–86) that has been shown to be important for IL-1 α association with the plasma membrane (24), MA-IL-1 is expected to express in Tg mice and play an important role in the development

*Department of Orthopedic Surgery, Keio University, Tokyo, Japan; [†]Department of Orthopedic Surgery, Fujita Health University, Aichi, Japan; [‡]Department of Orthopedic Surgery, National Defense Medical College, Saitama, Japan; and [§]Atopy Research Center, Juntendo University School of Medicine, Tokyo, Japan

Received for publication April 11, 2003. Accepted for publication October 24, 2003.

The costs of publication of this article were defrayed in part by the payment of page charges. This article must therefore be hereby marked *advertisement* in accordance with 18 U.S.C. Section 1734 solely to indicate this fact.

¹ Current address: Department of Orthopedic Surgery, Tokyo Women's Medical University, 10-22 Kawada-cho, Shinjuku-ku, Tokyo 162-0054, Japan.

² Address correspondence and reprint requests to Dr. Yasuo Niki, Department of Orthopedic Surgery, Keio University, 35 Shinanomachi, Shinjuku-ku, Tokyo 160-8582, Japan. E-mail address: y.niki@lib.bekkoame.ne.jp

³ Abbreviations used in this paper: RA, rheumatoid arthritis; hIL-1 α , human IL-1 α ; LMMA, L-N²-monomethyl arginine; MA-IL-1, membrane-associated IL-1; mL-1 α , mouse IL-1 α ; PFA, paraformaldehyde; PG, proteoglycan; Tg, transgenic.

of joint destruction. The present study investigated whether biologically active hIL-1 α derived from the transgene appears on the surface of synoviocytes, and whether MA-IL-1 contributes to synovial proliferation and cartilage destruction in the development of arthritis in hIL-1 α Tg mice. MA-IL-1 was found to be expressed on the surface of synoviocytes from Tg mice and triggered synovocyte self-proliferation and cartilage destruction *in vitro*. Interestingly, the activity of MA-IL-1, but not soluble IL-1, in synoviocytes displayed correlations with both macroscopic and histological severity of arthritis in Tg mice. These results suggest that blocking the activities of both membrane-associated and soluble IL-1 may be required to effectively neutralize the pathogenic potential of this cytokine in inflammatory arthropathy such as RA.

Materials and Methods

Generation of Tg mice

The generation of hIL-1 α Tg mice has been described previously (1). A 660-bp *HindIII/HincII* restriction fragment of hIL-1 α cDNA (Immunex, Seattle, WA) coding Lys⁶⁴ to Ala²⁷¹ of the hIL-1 α amino acid sequence was inserted into the *EcoRI* site of the third exon of the rabbit β -globin gene in the expression plasmid, pBsCAG-2. pBsCAG-2 possesses CAG containing the first intron of the chicken β -actin gene and a portion of the rabbit β -globin gene. The resulting construct was excised and microinjected into pronuclei of fertilized one-cell eggs from B6 \times B6C3F₁ mice. The established Tg mouse line (designated Tg1706) was backcrossed with C3H/HeJ mice for six to eight generations and used in all experiments. The Tg101 line, which was designed to integrate 420 bp of mature hIL-1 α cDNA coding Ser¹¹³ to Ala²⁷¹, was used in a histological examination, and the macroscopic and histological scores were compared with those of Tg1706 (Fig. 1).

Cell culture

Synovial specimens obtained from knee joints of 6- to 8-wk-old Tg mice were treated using 120 U/ml *Streptomyces sp.* C-51 collagenase (Sanko Junyaku, Tokyo, Japan) at 37°C for 30 min. Dispersed synovial cells were allowed to adhere to dishes in DMEM (Life Technologies, Gaithersburg, MD) containing 10% FBS (Life Technologies), 100 U/ml penicillin, and 100 μ g/ml streptomycin (Life Technologies). Fifth-passage cells were used in all experiments.

Macroscopic and histological assessment of arthritis

Clinical symptoms of arthritis in all four limbs were macroscopically evaluated according to a visual scoring system. Arthritic joints were graded on a scale of 0–4: 0 = no change, 0.5 = swelling and erythema of 1 digit, 1 = swelling and erythema of \geq 2 digits, 2 = mild swelling and erythema of the limb, 3 = gross swelling and erythema of the limb, and 4 = gross deformity and inability to use the limb. Scoring was performed in a blinded fashion by two observers, and the macroscopic score for each mouse comprised the sum of scores for all four limbs, for a maximum score of 16. In histological evaluations, ankle and knee joints were dissected and fixed in formalin. Sagittal sections (6 μ m) were prepared and stained using H&E. Using the method described by van den Berg et al. (25), synovial infiltration and cartilage destruction were scored on four semiserial sections of each specimen spaced 10 sections apart. Neutrophil infiltration was graded on a scale of 0–3, according to the number of neutrophils in synovial tissue. Cartilage destruction was also graded on a scale of 0–3: 0 = no change, 1 = dead chondrocytes (empty lacunae) or focal loss of cartilage,

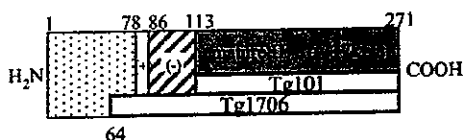


FIGURE 1. Schematic representation of human IL-1 α polypeptide. The transgenes of Tg1706 and Tg101 coded Lys⁶⁴ to Ala²⁷¹ and Ser¹¹³ to Ala²⁷¹ of human IL-1 α amino acid sequence, respectively: ▨, N-terminal conserved region (Met¹-Gly⁷⁸); □ (+), multiple basic region known as nuclear localization sequence (Lys⁷⁹-Arg⁸⁶); ▩ (-), negatively charged region (Leu⁸⁶-Arg¹¹²); ■, mature 17-kDa IL-1 α (Ser¹¹³-Ala²⁷¹).

2 = loss of 25–50% of cartilage, and 3 = complete loss of cartilage. Scoring was performed again in a blinded fashion by two observers, and histological scores for each mouse comprised the sum of scores for two hind limbs, for a maximum score of 24.

Flow cytometric analysis of MA-IL-1 synthesis

MA-IL-1 synthesis by synoviocytes was analyzed using flow cytometry. Briefly, adherent synoviocytes ($1-5 \times 10^5$ cells/test) were harvested and placed in ice-cold 5 mM EDTA and 1% BSA in Ca²⁺/Mg²⁺-free PBS at 37°C for 15 min. In accordance with the method described by Bailly et al. (26), either with or without 144 h of fixation in 1% (v/v) PFA at room temperature, synoviocytes were incubated for 15 min with unlabeled anti-CD16/32 (2.4G2; BD Pharmingen, San Diego, CA) to block nonspecific binding to FcR2/3. Cells were then stained using PE-labeled anti-hIL-1 α mAb (BD Immunocytometry Systems, San Jose, CA). In two-color analysis of freshly isolated synoviocytes, cells were further stained with biotinylated anti-F4/80 Ab (Cedarlane Laboratories, Hornby, Ontario, Canada), then incubated with cytochrome-conjugated streptavidin (BD Immunocytometry Systems). PE-conjugated mouse IgG (BD Pharmingen) was used as an isotype-matched control to exclude the possibility of nonspecific binding. Stained cells were then analyzed using FACScan (BD Biosciences, Mountain View, CA). In some experiments cells were treated with 0.01 μ g/ml trypsin before PFA fixation, then subjected to flow cytometry.

Immunoprecipitation of synovocyte membrane fraction

Cultured synoviocytes were maintained in methionine/cysteine-free medium (Life Technologies) for 2 h, then medium was replaced with freshly prepared appropriate deficient medium containing 40 μ Ci/ml [³⁵S]methionine/cysteine (Amersham Pharmacia Biotech, Little Chalfont, U.K.) for 6 h, and washed three times using ice-cold PBS. The synovocyte membrane fraction was prepared as previously described (27). Briefly, cultured synoviocytes harvested with ice-cold 5 mM EDTA in PBS were suspended at a concentration of 5×10^6 cells/ml in ice-cold homogenization buffer (20 mM Tris-HCl (pH 7.4), 10 mM NaCl, 0.1 mM MgCl₂, 0.1 mM PMSF, and 0.5 mg/ml DNase I), followed by sonication three times for 15 s each time. Homogenate was centrifuged at 95,000 \times g for 1 h over 41% (w/v) sucrose solution. The [³⁵S]methionine/cysteine-labeled membrane fraction was recovered from the interface and treated with lysis buffer (150 mM NaCl, 10 mM Tris-HCl (pH 7.5), 1% deoxycholate, 1% Triton X-100, 0.1% SDS, 10 mM EDTA, and 2 mM PMSF). This isolated membrane fraction was concentrated 5- to 10-fold in a Centricon Centrifugal Concentrator (Millipore, Bedford, MA), then subjected to immunoprecipitation with anti-hIL-1 α polyclonal Ab (Endogen, Woburn, MA) using an ImmunoPure Protein A IgG Orientation Kit (Pierce, Rockford, IL). In some experiments, 20 μ g of unlabeled recombinant hIL-1 α (Genzyme, Cambridge, MA) was added during immunoprecipitation. Labeled proteins in immunoprecipitates and ¹⁴C-methylated protein M_r marker (Amersham Pharmacia Biotech) were prepared for electrophoresis on 12.5% SDS-polyacrylamide gels, fixed, and treated with ENLIGHTNING (PerkinElmer, Boston, MA). Gels were dried and exposed to film at -80°C for autoradiography.

Bioassay for MA-IL-1 and soluble IL-1

MA-IL-1 bioactivity in synoviocytes was quantitated by PFA fixation of cells, as described by Bailly et al. (26). Briefly, synoviocytes were inoculated at 5×10^4 cells/well on 96-well, flat-bottom tissue culture plates (BD Biosciences, Franklin Park, NJ). After culturing for 24 h, cells were fixed with 1% PFA in PBS (pH 7.4) at room temperature for 144 h, washed three times, and incubated in 100 μ l of medium for 24 h. IL-1-sensitive mouse T cell clone D10.G4.1 (D10) cells (provided by Dr. Tadakuma, National Defense Medical College) were propagated as described previously (28), then used as an indicator for the presence of IL-1. In the synovocyte proliferation assay, Tg mouse-derived synoviocytes were used as indicators for IL-1. Indicator cells were distributed to wells at a concentration of 4×10^4 cells/well containing fixed synoviocytes in a total volume of 200 μ l of medium supplemented with 1 μ g/ml Con A (Sigma-Aldrich, St. Louis, MO). In assays for soluble IL-1, indicator cells were similarly distributed to wells in medium containing 25% (v/v) final concentration of samples, instead of fixed cells. The incorporation of [³H]thymidine into indicator cells was measured during the final 4 h of the 48-h culture. In some experiments neutralizing Abs against human IL-1 α (20 μ g/ml; Endogen) and/or mouse IL-1 α (20 μ g/ml; R&D Systems, Minneapolis, MN) were added to cultures during assays. Nonnal rabbit or goat IgGs (R&D Systems) were used as isotype-matched controls for anti-human or anti-mouse IL-1 α neutralizing Ab, respectively. The mitogenic activity of 100 μ g/ml

recombinant human IL-1 α (Endogen) was determined to provide a reference for the magnitude of the effects of MA-IL-1 expressed on fixed synoviocytes.

Effect of cell culture inserts on MA-IL-1 activity

Synoviocytes were inoculated at 1.5×10^5 cells/well on 24-well, flat-bottom tissue culture plates (BD Biosciences). After 24 h of culture, cells were fixed with 1% PFA in PBS (pH 7.4) at room temperature for 144 h. Live synoviocytes were added to wells as indicator cells at 1.5×10^5 cells/well in a total volume of 500 μ l, either directly or into the top compartment of the Cell Culture Insert (BD Biosciences). Incorporation of [3 H]thymidine into live synoviocytes was measured during the final 24 h of the 48-h culture. For blockade of IL-1, neutralizing Abs against hIL-1 α (20 μ g/ml; Endogen) and/or mouse IL-1 α (20 μ g/ml; R&D Systems) were added to cultures during assays.

Analysis of kinetics for synthesis of MA-IL-1 and soluble IL-1

Synoviocytes were inoculated at 1.5×10^5 cells/well on 24-well, flat-bottom plates (BD Biosciences) in a total volume of 500 μ l and incubated for 24, 48, 72, or 96 h, and culture supernatants were collected before fixation in 1% PFA for 144 h. In MA-IL-1 assays, 1.5×10^5 D10 cells were added to PFA-fixed synoviocytes. In soluble IL-1 assays, 1.5×10^5 D10 cells were incubated with a 25% (v/v) final concentration of culture supernatants from the corresponding time points. Incorporation of [3 H]thymidine into D10 cells was measured during the final 4 h of the 48-h culture.

Proteoglycan release assay

Articular chondrocytes were obtained from glenohumeral joints of young Japanese White rabbits. Freshly isolated chondrocytes were seeded at 1×10^5 cells/ml in a 24-well, flat-bottom plate (BD Biosciences). After 1 wk of culture, confluent cells were incubated for 24 h in 500 μ l of fresh medium containing [35 S]sulfate (Amersham Pharmacia Biotech) at 5 μ Ci/ml and washed four times with cold fresh medium. Radiolabeled cells were further incubated for 48 h in the presence or the absence of detergent-insoluble membrane fraction isolated from synoviocytes. In some wells, labeled cells were incubated with membrane fraction isolated from trypsin-treated synoviocytes or with 100 μ M L-N G -monomethyl arginine (L-NMMA; Wako Pure Chemical Industries, Osaka, Japan), an NO synthase inhibitor. The amount of [35 S]-labeled proteoglycan (PG) in cell and matrix layer and in supernatant was determined as previously described (29). Briefly, [35 S]-labeled cells and supernatants were separated. A total of 25 μ l of supernatant was solubilized using 75 μ l of 1.33 M guanidine HCl with 0.5% Triton X-100. Twenty-five microliters of [35 S]-labeled cell and matrix layer was solubilized for 4 h at 4°C with 4 M guanidine HCl and 0.05 M sodium acetate, pH 6.0, containing protease inhibitors, followed by dilution with 75 μ l of dilution buffer containing 0.5% Triton X-100. Next, 100 μ l of each sample was prepared in a 96-well MultiScreen filtration plate assembly (Millipore), and 150 μ l of 0.2% Alcian Blue was added to the well. Well contents were then filtered through the Millipore Durapore membrane (0.45- μ m pore size). Unincorporated [35 S]sulfate was removed by three passages of vacuum filtration with wash buffer through the membrane. The membrane disc in each well was punched out and applied to the scintillation counter. All samples were analyzed in triplicate. PG release into supernatant was calculated according to the following equation: % PG release = $\frac{[^{35}\text{S}]\text{PG in supernatant}}{[^{35}\text{S}]\text{PG in cell and matrix} + [^{35}\text{S}]\text{PG in supernatant}} \times 100\%$.

Statistical analysis

Results were expressed as the mean \pm SEM. Statistical comparisons were performed using nonparametric Mann-Whitney *U* tests. Correlation analysis was performed using StatView-J 5.0 statistical software (SAS Institute, Cary, NC). A value of $p < 0.05$ was considered statistically significant.

Results

Flow cytometric analysis of MA-IL-1

Two-color flow cytometric analysis of transgene-derived MA-IL-1 revealed that freshly isolated synoviocytes consisted of \sim 80% F4/80 $^+$ synovial macrophages and 20% F4/80 $^-$ synovial fibroblasts (Fig. 2A, left panel). In histogram analysis, \sim 78% of F4/80 $^+$ cells and 70% of F4/80 $^-$ cells expressed MA-IL-1 on their cell surface (Fig. 2A, right panel). As hIL-1 α Tg mice constitutively express transgene under the control of CAG promoter, both types of synoviocytes constitutively produced hIL-1 α . The fact that mem-

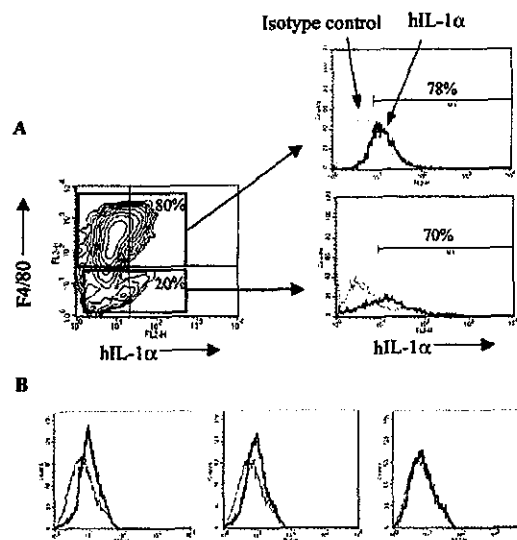


FIGURE 2. Flow cytometric analysis of transgene-derived MA-IL-1 on the surface of synoviocytes. *A*, Freshly isolated synoviocytes from 8-wk-old Tg mice were stained with PE-labeled anti-hIL-1 α Ab in conjunction with biotinylated anti-F4/80 Ab to identify synovial macrophages (*right panel*). The levels of MA-IL-1 after gating on F4/80 $^+$ cells or F4/80 $^-$ cells are shown in histograms. The percentage of cells expressing MA-IL-1 is indicated (*right panel*). The results are representative of three different experiments. *B*, MA-IL-1 expression in fifth-passage synoviocytes (purity of synovial fibroblasts, $>95\%$). Histograms show effects of PFA-fixation and mild trypsin treatment on the staining pattern of cell surface hIL-1 α . MA-IL-1 can be detected on the surface of synoviocytes in both the presence (*middle panel*) and absence (*left panel*) of PFA fixation. MA-IL-1 exposed on the surface of synoviocytes was removed by mild trypsin treatment (*right panel*). Gray lines show the background with isotype-matched control Abs. Results are representative of three different experiments.

brane permeabilization was not required for staining synoviocytes with PE-labeled hIL-1 α Ab ensured cell surface distribution of hIL-1 α (Fig. 2B, left panel). Identical staining patterns were observed in PFA-fixed synoviocytes (Fig. 2B, middle panel). Furthermore, this membrane-localized IL-1 in synoviocytes was removed with mild trypsin treatment (Fig. 2B, right panel), as reported by others (9, 30). This indicates that MA-IL-1 was substantially anchored in the membrane, with tryptic cleavage sites exposed on the cellular surface.

Immunoprecipitation of MA-IL-1

To further confirm membrane localization of transgene-derived hIL-1 α , a membrane fraction was isolated from synoviocytes, and immunoprecipitation was performed using specific Abs. The results clearly indicated that transgene-derived hIL-1 α within the membrane fraction included a 25-kDa protein, slightly heavier than the 23-kDa primary translation product of the transgene (Fig. 3). In fact, culture supernatants and cell lysates of synoviocytes displayed both 23- and 25-kDa hIL-1 α proteins (1). However, only the 25-kDa protein was detected in the membrane fraction. This preferential distribution of 25-kDa hIL-1 α implies the promotion of post-translational modifications probably related to membrane localization of hIL-1 α , such as phosphorylation (5), mannosylation (6), and myristoylation (7). To examine whether this band was the truth, competition analysis was performed by adding excess unlabeled recombinant hIL-1 α (\sim 2.0 μ g) during immunoprecipitation. As expected, recombinant hIL-1 α completely prevented the immunoprecipitation of labeled hIL-1 α with specific Ab, whereas neither recombinant hIL-1 β nor mouse IL-1 α (mIL-1 α) demonstrated any

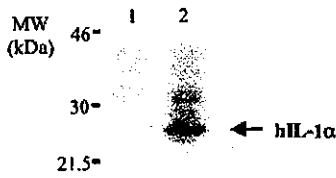


FIGURE 3. Immunoprecipitation of hIL-1 α isolated from synoviocyte membrane fraction. Cultured synoviocytes were labeled with [35 S]methionine/cysteine (40 μ Ci/ml) for 6 h. Membrane fraction was obtained as indicated in *Materials and Methods*, followed by immunoprecipitation using anti-hIL-1 α polyclonal Ab. *Lane 1*, Immunoprecipitation in the presence of excess unlabeled recombinant hIL-1 α . *Lane 2*, immunoprecipitation of synoviocyte membrane fraction, showing the 25-kDa precursor form of hIL-1 α (arrow).

effect (data not shown). This indicates that transgene-derived hIL-1 α actually localizes within the membrane of synoviocytes.

MA-IL-1 on the surface of synoviocytes is biologically active and promotes synoviocyte proliferation

Kaye and co-workers (31, 32) have reported a IL-1-sensitive T cell clone, D10.G4.1, that can be used to detect and titrate IL-1 by adding test molecules together with Con A. Using these characteristics of D10 cells, MA-IL-1 expression on LPS-stimulated macrophages has been elucidated by [3 H]thymidine incorporation into D10 cells cultured on PFA-fixed macrophages (14). This procedure was used to determine the MA-IL-1 activity of synoviocytes from Tg mice. Tg mouse-derived synoviocytes significantly

stimulated D10 cell proliferation compared with littermate-derived synoviocytes (Fig. 4A). To exclude the possibility of the mitogenic activity of MA-IL-1 actually being attributable to minor contaminants in preparations, neutralizing Ab against hIL-1 α /mIL-1 α was added to cultures during the assay. Addition of anti-hIL-1 α Ab resulted in significant inhibition of D10 cell proliferation, suggesting that bioactivity of synoviocytes is due to transgene-derived MA-IL-1. Furthermore, anti-mIL-1 α Ab inhibited D10 cell proliferation to a similar degree as anti-hIL-1 α Ab, with inhibition reaching a maximum with the combination of both Abs. Transgene-derived MA-IL-1 thus induces the production of endogenous mouse MA-IL-1, and both forms of MA-IL-1 may play a role in the development of proliferative synovitis in Tg mice. As IL-1 has been shown to act as a mitogen for synoviocytes (33–35), the effects of MA-IL-1 on synoviocyte proliferation were examined. In this experiment, live synoviocytes isolated from Tg mice and RA patients were used as indicator cells for IL-1 activity, instead of D10 cells. Notably, putative MA-IL-1 in Tg mouse-derived synoviocytes led to significant stimulation of [3 H]thymidine incorporation into indicator cells compared with that in littermate-derived synoviocytes (Fig. 4B), indicating that MA-IL-1 on Tg mouse-derived synoviocytes stimulates synoviocyte self-proliferation via juxtacrine mechanisms.

MA-IL-1 expression and its activity affect severity of arthritis in Tg mice

To elucidate the contribution of MA-IL-1 to the development of arthritis, the severity of arthritis was evaluated according to a scoring system. Clinical symptoms of arthritis in all four paws and histology of bilateral knee joints were scored, and these macroscopic and histological scores were compared between the two Tg mouse lines, Tg1706 and Tg101, which overexpress pro-IL-1 α and mature IL-1 α , respectively. Interestingly, these scores of Tg1706

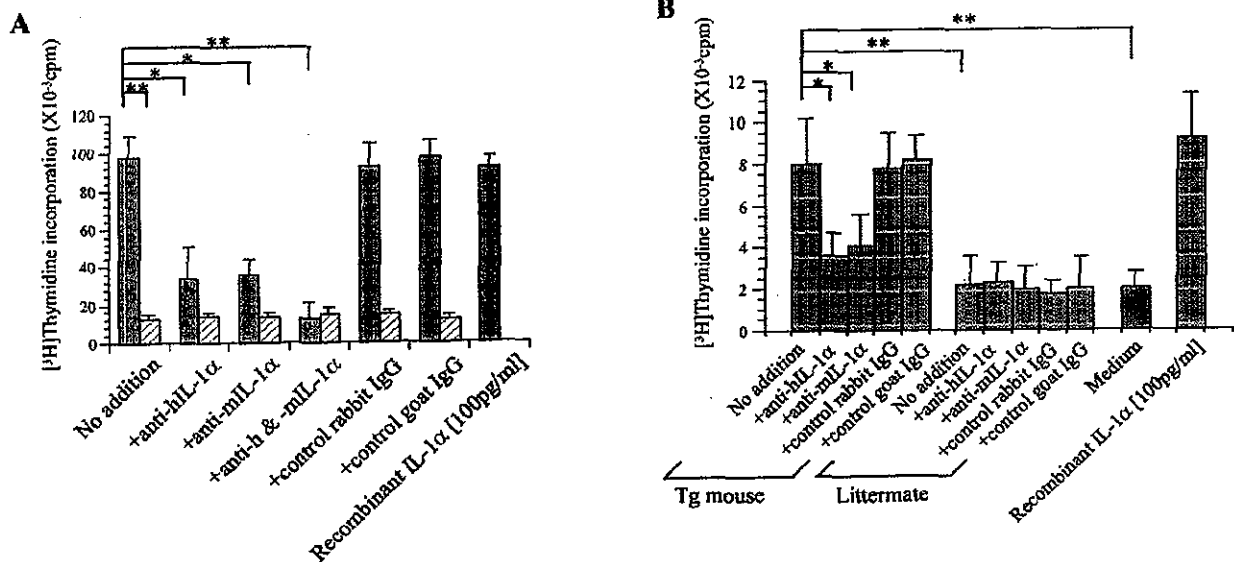


FIGURE 4. *A*, Tg mouse-derived synoviocytes express biologically active MA-IL-1. Fifth-passage synoviocytes isolated from Tg mouse (■) or littermates (▨) were inoculated on 96-well plates and fixed with 1% PFA in PBS for 144 h. D10 cells were distributed to wells and incubated with or without neutralizing Abs against hIL-1 α /mIL-1 α . Isotype-matched control IgGs were used to exclude a possibility that these neutralizations include nonspecific reactions. [3 H]thymidine incorporation into D10 cells was measured during the final 4 h of a 48-h incubation. Data represent the mean counts per minute \pm SEM of four separate experiments. *B*, MA-IL-1 contributes to self-proliferation of synoviocytes. Tg mouse- or littermate-derived synoviocytes cultured on 96-well plates were fixed with 1% PFA for 144 h. Live synoviocytes from Tg mouse were overlaid on the fixed cells with or without neutralizing Abs against hIL-1 α /mIL-1 α . [3 H]thymidine incorporation into overlaid synoviocytes was measured during the final 4 h of a 48-h incubation. Control comprised [3 H]thymidine incorporation into synoviocytes incubated with medium alone. Data represent the mean counts per minute \pm SEM of four separate experiments. *, $p < 0.05$; **, $p < 0.01$.

were significantly higher than those of Tg101, indicating relatively severe arthritic phenotype in Tg1706 compared with Tg101 (Fig. 5A). In the next experiment, the relationship between MA-IL-1 activity of synoviocytes and severity of arthritis was examined in 10 6-wk-old Tg mice. Correlations between these scores and levels of MA-IL-1, soluble IL-1, and serum hIL-1 α were determined. Linear analyses revealed that MA-IL-1 activity displayed significant correlations with both macroscopic and histological scores (Fig. 5B). However, soluble IL-1 activity and serum concentrations of hIL-1 α displayed no correlation with either score. MA-IL-1 expression in synovial tissue may therefore represent a key element in the development of synovitis and subsequent joint destruction in Tg mice.

Direct cell-to-cell contact is indispensable in promotion of MA-IL-1 activity

To investigate whether direct cell-to-cell interactions are required for MA-IL-1 activity, a coculture system using the cell culture insert with 1- μ m pores was employed, allowing the infiltration of macromolecules, but not direct cell-to-cell contact. Similar to the experiment in Fig. 5B, live synoviocytes were used as indicator cells for IL-1 activity and cocultured with PFA-fixed synoviocytes

with or without cell culture inserts. Significant differences in live synoviocyte proliferation were observed between the two different cultures. Live synoviocytes displayed obvious proliferation when directly cultured with PFA-fixed synoviocytes without separation (Fig. 6). However, once cells were separated from each other using a cell culture insert, the proliferative activity of PFA-fixed synoviocytes was abrogated. When neutralizing Abs against hIL-1 α /mIL-1 α were added to cultures during the assay, synoviocyte proliferation was significantly diminished in culture without cell culture insert, indicating that this proliferative activity was attributable to MA-IL-1 in PFA-fixed synoviocytes. Weak, but nonsignificant, neutralization was observed in culture with the cell culture insert; in contrast to D10 cells, Tg mouse-derived synoviocytes spontaneously produce soluble IL-1 and MA-IL-1, and endogenous IL-1-dependent proliferation of these cells was blocked by the specific Abs. These results indicate that direct cell-to-cell contact is indispensable in the promotion of proliferative activity by MA-IL-1.

Differential kinetics between synthesis of MA-IL-1 and soluble IL-1

To investigate the kinetics of synthesis for MA-IL-1 and soluble IL-1, incorporation of [³H]thymidine into synoviocytes was determined when cells were overlaid on PFA-fixed synoviocytes as a

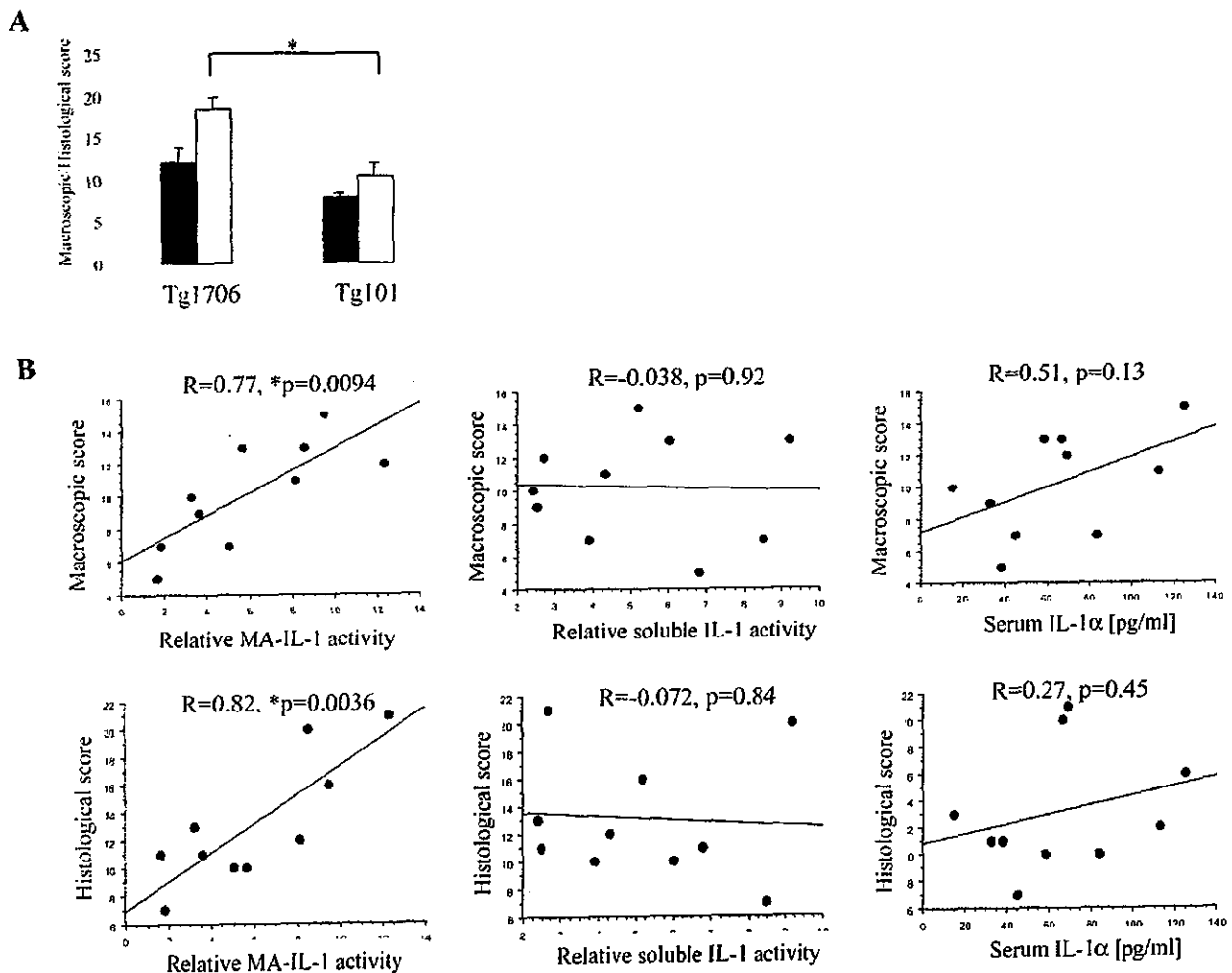


FIGURE 5. A, Comparison of severity of arthritis between Tg1706 and Tg101. Macroscopic and histological findings were scored at 6-wk-old Tg mice. Data are presented as the mean + SEM of four mice. B, Correlation between macroscopic score, histological score, relative MA-IL-1 activity, relative soluble IL-1 activity, and serum hIL-1 α level in 10 6-wk-old Tg mice. Data are presented as the coefficient (R) and p value derived from linear regression analysis. *, $p < 0.05$.

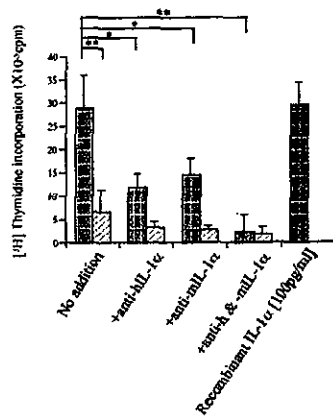


FIGURE 6. MA-IL-1 promotes synoviocyte proliferation in a cell-to-cell contact-dependent manner. Tg mouse-derived synoviocytes cultured on 24-well plates were fixed with 1% PFA for 144 h. Live synoviocytes were added directly to the fixed synoviocytes (■) or the top compartment of the cell culture insert (▨) and incubated for 48 h. For blockade of IL-1 activity, neutralizing Abs against hIL-1 α /mIL-1 α were added during incubation. [3 H]Thymidine incorporation into live synoviocytes was determined during the final 4 h of a 48-h incubation. Data are presented as the mean counts per minute \pm SEM for four separate experiments. *, $p < 0.05$; **, $p < 0.01$.

feeder layer of MA-IL-1. Soluble IL-1 secreted into culture supernatant by overlaid synoviocytes was demonstrable from 24 h after inoculation and plateaued between 72 and 96 h (Fig. 7A), whereas the corresponding MA-IL-1 activity reached a plateau by 24 h after inoculation, remaining stable until at least 96 h (Fig. 7B). In addition, the proliferative activity of soluble IL-1 was \sim 5-fold higher than that of MA-IL-1.

MA-IL-1 induces PG release from cartilage matrix in vitro

Monolayer-cultured articular chondrocytes derived from Japanese White rabbits were labeled with [35 S]sulfate for 24 h, then incubated with synoviocyte membrane fraction in the presence or the absence of anti-hIL-1 α Ab for 48 h. Release of [35 S]-labeled PG from cell and matrix layer was examined. The synoviocyte membrane fraction significantly stimulated PG release into culture supernatant compared with control (Fig. 8), and stimulation was decreased almost to control levels by the addition of anti-IL-1 α Ab. In contrast, the membrane fraction isolated from synoviocytes

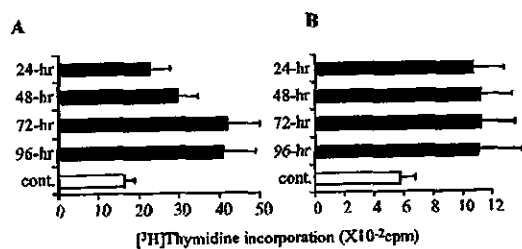


FIGURE 7. Synthetic kinetics of MA-IL-1 and soluble IL-1 α . Fifth-passage synoviocytes derived from Tg mice were fixed on the indicated day of culture after inoculation. Corresponding culture supernatants were collected immediately before fixation of synoviocytes. D10 cells were incubated on fixed cells or with a 25% (v/v) final concentration of culture supernatants. The IL-1 activity of supernatants (A) and fixed cells (B) was determined by measuring [3 H]thymidine incorporation into D10 cells during the last 4 h of a 48-h incubation (■). Control data for synoviocytes were derived from littermates (□). Data are presented as the mean counts per minute \pm SEM for four separate experiments.

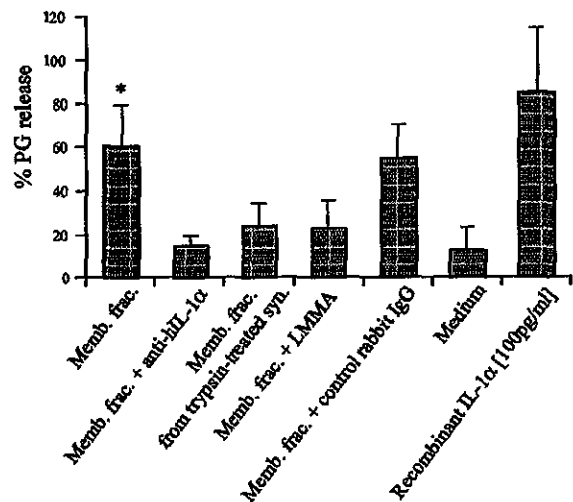


FIGURE 8. MA-IL-1 stimulates PG release from cartilage matrix through generation of NO. Cultured articular chondrocytes were radiolabeled with [35 S]sulfate for 24 h, then incubated for 48 h with synoviocyte membrane fraction alone, membrane fraction plus anti-hIL-1 α Ab, membrane fraction plus 100 mM LMMA, or membrane fraction isolated from trypsin-treated synoviocytes. Control data were derived from chondrocytes without membrane fraction. The release of [35 S]-labeled PG from the cell and matrix layer to culture supernatant was examined. The percent PG release was calculated according to the following equation: % release = [35 S]PG in supernatant/[35 S]PG in cell and matrix + [35 S]PG in supernatant. Data are presented as the mean counts per minute \pm SEM for four separate experiments. *, $p < 0.05$ compared with the control.

treated with mild trypsin did not affect PG release, compatible with the flow cytometric data in Fig. 3C showing that MA-IL-1 has a tryptic cleavage site and can be removed by mild trypsin treatment. Furthermore, the NO synthase inhibitor, LMMA, for the most part inhibited membrane fraction-stimulated PG release, indicating the involvement of NO in this process. These data suggest that MA-IL-1 induces PG release from the cell and matrix through generating NO in chondrocyte monolayer culture, further indicating that MA-IL-1 may play a role in cartilage destruction in vivo.

Discussion

MA-IL-1 was found to play key roles in the development of arthritic phenotypes in Tg mice. Of interest is the fact that both macroscopic and histological scores were correlated with activity of MA-IL-1, but not with activity of soluble IL-1 produced by synoviocytes. Moreover, cartilage destruction of Tg101 line overexpressing 17-kDa mature IL-1 α was relatively mild even at 12 wk after birth, although the Tg1706 line overexpressing pro-IL-1 α demonstrated complete loss of cartilage at 8 wk after birth, which reflected low macroscopic and histological scores in the Tg101 line. This observation was not attributable to the difference in levels of serum IL-1 α were almost similar (\sim 100 pg/ml). Thus, as in Tg mouse studies on membrane-associated TNF (36, 37), the arthritogenic properties of MA-IL-1 may be sufficient to cause severe arthritis even in conditions without processing of proteins to mature form.

However, we cannot neglect the fact that, in general, transgene expression can be affected by copy number and integration site of the transgene, and a simple comparative study of phenotypic characteristics among Tg mouse lines is unlikely to provide informative data. In actual fact, we established two transgenic founders for

each Tg mouse for pro- and active IL-1 α . As assessed by tail Southern blot analysis, copy number of transgenes was similar among the four transgenic founders (three or four copies), and differences in integration site were confirmed by fluorescence in situ hybridization analysis. Northern blot analysis revealed quite similar levels and patterns of mRNA expression in all four transgenic founders, and of course in offspring of Tg101 and Tg1706. All four founders exhibited arthritic phenotypes, and a more severe arthritic phenotype in pro-IL-1 α Tg mice than in active IL-1 α Tg mice was noted as a universal trend, even in offspring. This indicates that in our study the effects of copy number and integration site of transgenes can be neglected, allowing direct comparison of the two Tg mouse lines. We therefore believe that Tg mice for pro-IL-1 α exhibited a more progressive arthritic phenotype than mice for active IL-1 α , and membrane IL-1 plays an important role in the evolution of inflammatory arthritis.

To date, MA-IL-1 has been shown to be more potent than soluble IL-1 in a variety of situations, such as neutrophil extravasation via endothelial cells, T cell activation during Ag presentation, and osteoclast formation through up-regulation of receptor activator NF- κ B ligand expression on osteoblasts, all of which play crucial roles in the development of inflammatory joint diseases. Of the pleiotropic activities of MA-IL-1, the present study focused on the effects on synoviocytes and chondrocytes, as IL-1 has been shown to act as a mitogen for rheumatoid synovial fibroblasts, and abnormal IL-1 production contributes to synovial proliferation and degradation of the cartilage matrix in RA and collagen-induced arthritis in mice. As MA-IL-1 synthesis is spontaneously promoted in hIL-1 α Tg mice and persists due to the characteristics of the promoter, synoviocytes cultured on PFA-fixed synoviocytes displayed marked proliferation in the absence of stimuli. Moreover, transgene-derived hIL-1 α further up-regulated endogenous mouse MA-IL-1 synthesis via autocrine mechanisms, and this may also be involved in the joint pathology of hIL-1 α Tg mice.

Kurt-Jones et al. (12) provided the first evidence that PFA-fixed macrophages stimulate IL-1-sensitive T cell clone, D10 G4.1 proliferation due to IL-1 activity on the external plasma membrane of macrophage. In the present study MA-IL-1 expression on the surface of synoviocytes isolated from arthritic joints was directly identified using flow cytometry. Cellular staining regardless of membrane permeabilization and dissociation of hIL-1 α from the cell surface by mild trypsin treatment indicated that IL-1 α is undoubtedly associated with the exterior plasma membrane surface of synoviocytes. Matsushima et al. (30) also documented the release of biologically active IL-1 from plasma membrane, when LPS-stimulated macrophages are treated with mild trypsin or plasmin-like proteases.

IL-1 α precursor propeptide lacks a classical signal sequence (4), which is known to regulate the processing of secreted and integral plasma membrane-associated proteins. To date, a number of post-translational modifications within the NII₂-terminal domain have been proposed to affect the intracellular distribution of IL-1 α , including phosphorylation (5), mannosylation (6), and myristoylation (7). However, the details of these processes have remained unknown. Several speculations have been proposed regarding such post-translational modifications and their impact on intracellular distribution of IL-1 α . One investigator has demonstrated that phosphorylation of newly synthesized IL-1 α signifies intracellular routing of IL-1 α precursor, and ~10% of phosphorylated IL-1 α precursor is committed to the membrane-associated form. Another study revealed that glycosylation of IL-1 α precursor allows association with membrane-bound lectins and membrane-localization of IL-1 α (6). Alternatively, striking evidence has been proposed that physical injury or programmed cell death (i.e., apoptosis) play

a role in IL-1 α secretion through membrane disruption (38). Although certain post-translational modifications are likely to reflect the difference between transgene-predicted (25 kDa) and observed (23 kDa) masses of IL-1 α precursor in immunoprecipitation of the synoviocyte membrane fraction in IL-1 α Tg mice, the mechanisms affecting membrane localization of IL-1 α remain unknown.

MA-IL-1 expression on the surface of synoviocytes was clarified from another perspective. Synoviocytes were plated onto 24-well plates and fixed using 1% PFA. Live synoviocytes were directly added to fixed synoviocytes or the top compartment of the cell culture insert, allowing soluble IL-1 α , but not MA-IL-1, to migrate between the top and bottom compartments. This experiment indicated that synoviocytes without separation engaged in direct cell-to-cell interactions, resulting in higher proliferation attributable to the activities of soluble IL-1 plus MA-IL-1. However, the true magnitude of [³H]thymidine incorporation into indicator synoviocytes cultured on the PFA-fixed synoviocytes actually appeared higher than that cultured on nonfixed live synoviocytes. This can be explained by our unpublished observations that live synoviocytes spontaneously produce IL-1 receptor antagonist *in vitro*, which may block IL-1 activity during the experiment.

As reported by van de Loo et al. (39, 40), IL-1 inhibits synthesis of PG by chondrocytes through generation of NO in zymosan-induced arthritis. The present study demonstrated that membrane fraction isolated from synoviocytes induces PG release from the cartilage matrix in chondrocyte monolayer culture, and that this phenomenon is mediated by NO synthesis. This indicates that MA-IL-1 within the membrane is essentially implicated in chondrocyte PG loss, suggesting the possibility that MA-IL-1 contributes to cartilage destruction during the course of arthritis in IL-1 α Tg mice. However, PG loss was not detected when chondrocytes were cultured in agarose gels (data not shown). The absence of chondrocyte PG loss is probably attributable to the prevention of direct cell-to-cell contact by the surrounding agarose gel. Chondrocyte PG loss caused by the synoviocyte membrane fraction may thus, for the most part, be due to MA-IL-1 within the membrane.

Finally, the importance of membrane-associated molecules proposed in the current experimental study is that cell-cell interactions between macrophage-like synoviocytes and T lymphocytes activate the production of proinflammatory cytokines at the inflamed synovium (41–43). These include membrane-associated IL-1 and TNF, which induce fibroblast-like synoviocytes to produce large amounts of matrix metalloproteinases that degrade cartilage and bone. In the present study using IL-1 α Tg mice, MA-IL-1 expressed on synoviocytes may trigger synoviocyte self-proliferation and induce cartilage degradation, mechanisms that may operate in the cartilage-pannus junction through cell-cell interactions *in vivo*. Moreover, a correlation between MA-IL-1 activity and severity of arthritis indicates that MA-IL-1 is a potent effector of joint inflammation. As the present results were obtained purely from animal studies, the importance and extent of MA-IL-1 contribution to the pathogenesis of human inflammatory joint diseases such as RA warrant investigation.

Acknowledgments

We are grateful to the late Prof. Masayuki Shinmei (Department of Orthopedic Surgery, National Defense Medical College) for the planning of this investigation. We also thank Prof. Takushi Tadakuma (Department of Parasitology, National Defense Medical College) for providing the D10.G4.1 cells used in this study.

References

1. Niki, Y., H. Yamada, S. Seki, T. Kikuchi, H. Takaishi, Y. Toyama, K. Fujikawa, and N. Tada. 2001. Macrophage- and neutrophil-dominant arthritis in human IL-1 α transgenic mice. *J. Clin. Invest.* 107:1127.

2. March, C. J., B. Mosley, A. Larsen, D. P. Cerretti, G. Braedt, V. Price, S. Gillis, C. S. Henney, S. R. Kronheim, and K. Grabstein. 1985. Cloning, sequence and expression of two distinct human interleukin-1. *Nature* 315:641.
3. Mostley, B., D. L. Urdal, K. S. Prickett, A. Larsen, D. Cosman, P. J. Conlon, S. Gillis, and S. K. Dower. 1987. The interleukin-1 receptor binds to the human interleukin-1 α precursor but not the interleukin-1 β precursor. *J. Biol. Chem.* 262:2941.
4. Dinarello, C. A. 1996. Biologic basis for interleukin-1 in disease. *Blood* 87:2095.
5. Beuscher, H. U., M. W. Nickells, and H. R. Colten. 1988. The precursor of interleukin-1 α is phosphorylated at residue serine 90. *J. Biol. Chem.* 263:4023.
6. Brody, D. T., and S. K. Durum. 1989. Membrane IL-1: IL-1 α precursor binds to the plasma membrane via a lectin-like interaction. *J. Immunol.* 143:1183.
7. Stevenson, F. T., S. J., Bursten, C. Fanton, R. M. Locksley, and D. H. Lovett. 1993. The 31-kDa precursor of interleukin-1 α is myristoylated on specific lysines within the 16-kDa N-terminal propeptide. *Proc. Natl. Acad. Sci. USA* 90:7245.
8. Carruth, L., S. Demczuk, and S. Mizel. 1991. Involvement of a calpain-like protease in the processing of the murine interleukin-1 α precursor. *J. Biol. Chem.* 266:12162.
9. Kobayashi, Y., K. Yamamoto, T. Saido, H. Kawasaki, and J. J. Oppenheim. 1990. Identification of calcium-activated neutral protease as a processing enzyme of human interleukin 1 α . *Proc. Natl. Acad. Sci. USA* 87:5548.
10. Lee, R. T., W. H. Briggs, G. C. Cheng, H. B. Rossiter, P. Libby, and T. Kupper. 1997. Mechanical deformation promotes secretion of IL-1 α and IL-1 receptor antagonist. *J. Immunol.* 159:5084.
11. Conlon, P. J., K. H. Grabstein, A. Alpert, K. S. Prickett, T. P. Hopp, and S. Gillis. 1987. Localization of human mononuclear cell interleukin 1. *J. Immunol.* 139:98.
12. Kurt-Jones, E. A., D. I. Beller, S. B. Mizel, and E. R. Unanue. 1985. Identification of a membrane-associated interleukin-1 in macrophages. *Proc. Natl. Acad. Sci. USA* 82:1204.
13. Junning, L. E., D. Weinstein, U. Gubler, and J. Vilcek. 1987. Induction of membrane-associated interleukin 1 by tumor necrosis factor in human fibroblasts. *J. Immunol.* 138:2137.
14. Kurt-Jones, E. A., W. Fiers, and J. S. Pober. 1987. Membrane interleukin 1 induction on human endothelial cells and dermal fibroblasts. *J. Immunol.* 139:2317.
15. Zola, H., L. Flego, Y. T. Wong, P. J. Macardle, and J. S. Kenney. 1993. Direct demonstration membrane IL-1 α on the surface on circulating B lymphocytes and monocytes. *J. Immunol.* 150:1755.
16. Yamashita, U., F. Shirakawa, and H. Nakamura. 1987. Production of interleukin 1 by adult T cell leukemia (ATL) cell lines. *J. Immunol.* 138:3284.
17. Acres, R. B., A. L. F. Larsen, and P. J. Conlon. 1987. IL 1 expression in a clone of human T cells. *J. Immunol.* 138:2132.
18. Nishimura, T., Y. Ishihara, T. Noguchi, and T. Koga. 1989. Membrane IL-1 induces bone resorption in organ culture. *J. Immunol.* 143:1881.
19. Kaplanski, G., R. Porat, K. Aïra, J. K. Erban, and C. A. Dinarello. 1993. Activated platelets induce endothelial secretion of interleukin-8 in vitro via an interleukin-1-mediated event. *Blood* 81:2492.
20. Beasley, D., and A. L. Cooper. 1999. Constitutive expression of interleukin-1 α precursor promotes human vascular smooth muscle cell proliferation. *Am. J. Physiol.* 276:H901.
21. Weaver, C. T., and E. R. Unanue. 1986. T cell induction of membrane IL-1 on macrophages. *J. Immunol.* 137:3868.
22. Suresh, A., and A. Sodhi. 1991. Production of interleukin-1 and tumor necrosis factor by bone marrow-derived macrophages: effect of cisplatin and lipopolysaccharide. *Immunol. Lett.* 30:93.
23. Nishihara, T., T. Takahashi, Y. Ishihara, H. Senpuku, and T. Koga. 1994. Membrane-associated interleukin-1 promotes osteoclast-like cell formation in vitro. *Bone Miner.* 25:15.
24. McMahon, G. A., S. Garfinkel, I. Prudovsky, X. Hu, and T. Maciag. 1997. Intracellular precursor interleukin (IL)-1 α , but not mature IL-1 α , is able to regulate human endothelial cell migration in vitro. *J. Biol. Chem.* 272:28202.
25. van den Berg, W. B., L. A. B. Joosten, M. Helsen, and F. A. J. van de Loo. 1994. Amelioration of established murine collagen-induced arthritis with anti-IL-1 treatment. *Clin. Exp. Immunol.* 95:237.
26. Bailly, S., B. Ferrua, M. Fay, and M. A. Gougerot-Pocidalo. 1990. Paraformaldehyde fixation of LPS-stimulated human monocytes: technical parameters permitting the study of membrane IL-1 activity. *Eur. Cytokine Network* 1:47.
27. Maeda, T., K. Balakrishnan, and Q. Mehdi. 1983. A simple and rapid method for the preparation of plasma membranes. *Biochim. Biophys. Acta* 731:115.
28. Helle, M., L. Boeije, and L. A. Aarden. 1988. Functional discrimination between interleukin 6 and interleukin 1. *Eur. J. Immunol.* 18:1535.
29. Masuda, K., H. Shirota, and E. J. M. A. Thonar. 1994. Quantification of ³⁵S-labeled proteoglycans complexed to Alcian Blue by rapid filtration in multiwell plates. *Anal. Biochem.* 217:167.
30. Matsushima, K., M. Taguchi, E. J. Kovacs, H. A. Young, and J. J. Oppenheim. 1986. Intracellular localization of human monocyte associated interleukin 1 (IL 1) activity and release of biologically active IL 1 from monocytes by trypsin and plasmin. *J. Immunol.* 136:2883.
31. Kaye, J., S. Porcelli, J. Tite, B. Jones, and C. A. Janeway, Jr. 1983. Both a monoclonal antibody and antisera specific for determinants unique to individual cloned helper T cell lines can substitute for antigen and antigen-presenting cells in the activation of T cells. *J. Exp. Med.* 158:836.
32. Kaye, J., S. Gillis, S. B. Mizel, E. M. Shevach, T. R. Malek, C. A. Dinarello, L. B. Lachman, and C. A. Janeway, Jr. 1984. Growth of a cloned helper T cell line induced by a monoclonal antibody specific for the antigen receptor: interleukin 1 is required for the expression of receptors for interleukin 2. *J. Immunol.* 133:1339.
33. Rupp, E. A., P. M. Cameron, C. S. Ranawat, J. A. Schmidt, and B. K. Bayne. 1986. Specific bioactivities of monocyte-derived interleukin-1 α and interleukin-1 β are similar to each other on cultured murine thymocytes and on cultured human connective tissue cells. *J. Clin. Invest.* 78:836.
34. Alvaro-Gracia, J. M., N. J. Zvaifler, and G. S. Firestein. 1990. Cytokines in chronic inflammatory arthritis. V. Mutual antagonism between interferon-gamma and tumor necrosis factor- α on HLA-DR expression, proliferation, collagenase production and granulocyte macrophage colony-stimulating factor production by rheumatoid arthritis synovial cells. *J. Clin. Invest.* 86:1790.
35. Butler, D. M., D. S. Piccoli, P. H. Hart, and J. A. Hamilton. 1988. Stimulation of human synovial fibroblast DNA synthesis by recombinant human cytokines. *J. Rheumatol.* 15:1463.
36. Probert, L., K. Akassoglou, L. Alexopoulos, E. Douni, S. Haralambous, S. Hill, G. Kassiotis, D. Kontoyiannis, M. Pasparakis, D. Plows, et al. 1996. Dissection of the pathologies induced by transmembrane and wild-type tumor necrosis factor in transgenic mice. *J. Leukocyte Biol.* 59:518.
37. Georgopoulos, S., D. Plows, and G. Kollias. 1996. Transmembrane TNF is sufficient to induce localized tissue toxicity and chronic inflammatory arthritis in transgenic mice. *J. Inflamm.* 46:86.
38. Hogquist, K. A., M. A. Nett, E. R. Unanue, and D. D. Chaplin. 1991. Interleukin 1 is processed and released during apoptosis. *Proc. Natl. Acad. Sci. USA* 88:8485.
39. van de Loo, A. A. J., and W. B. van den Berg. 1990. Effects of murine recombinant IL-1 on synovial joints in mice: quantification of patellar cartilage metabolism and joint inflammation. *Ann. Rheum. Dis.* 49:238.
40. Van de Loo, F. A. J., O. J. Arntz, F. H. J. van Enekevort, P. L. E. M. van Lent, and W. B. van den Berg. 1998. Reduced cartilage proteoglycan loss during zymosan-induced gonarthrosis in NOS2-deficient mice and in anti-interleukin-1-treated wild-type mice with unabated joint inflammation. *Arthritis Rheum.* 41:634.
41. Seckinger, P., M. T. Kaufmann, and J. M. Dayer. 1990. An Interleukin 1 inhibitor affects both cell-associated interleukin 1-induced T cell proliferation and PGE₂/collagenase production by human dermal fibroblasts and synovial cells. *Immunobiology* 180:316.
42. Burger, D., R. Rezzonico, H. M. C. Modoux, R. A. Pierce, H. G. Welgus, and J. M. Dayer. 1998. Imbalance between interstitial collagenase and tissue inhibitor of metalloproteinases 1 in synovial cells and fibroblasts upon direct contact with stimulated T lymphocytes: involvement of membrane-associated cytokines. *Arthritis Rheum.* 41:1748.
43. Burger, D., and J. M. Dayer. 1999. Cytokines and direct cell contact in synovitis: relevance to therapeutic intervention. *Arthritis Res.* 1:17.

Osteopontin is Strongly Expressed by Alveolar Macrophages in the Lungs of Acute Respiratory Distress Syndrome

Fumiyuki Takahashi,^{1,2} Kazuhisa Takahashi,^{1,2} Kazue Shimizu,^{1,2} Ri Cui,^{1,2} Norihiro Tada,³ Hidcki Takahashi,^{1,2} Sanac Soma,^{1,2} Masakata Yoshioka,^{1,2} and Yoshinosuke Fukuchi^{1,2}

¹Department of Respiratory Medicine, Juntendo University School of Medicine, Hongo, Bunkyo-Ku, Tokyo, Japan; ²Research Institute for Diseases of Old Ages, Tokyo, Japan; ³Atopy Research Center, Juntendo University, School of Medicine, 2-1-1 Hongo, Bunkyo-Ku, Tokyo 113-8421, Japan

Abstract. Acute respiratory distress syndrome (ARDS) is characterized by an intense inflammatory response in the lung parenchyma. Recent studies suggest that excessive nitric oxide (NO) production mediated by inducible NO synthase (iNOS) in macrophages is partially involved in mediating acute lung injury in ARDS. On the other hand, osteopontin (OPN) is a cytokine which is capable of inhibiting NO production by suppressing iNOS mRNA expression in macrophages. In this study, we investigated the expression of OPN in the lungs of 10 patients with ARDS. In most patients, OPN is strongly expressed on alveolar macrophages. In addition, we produced a murine model for ARDS by intratracheal administration of lipopolysaccharide and investigated the expression of endogenous OPN and iNOS in the lungs of ARDS mice. Immunostaining demonstrated that *in vivo* OPN protein was coinduced with iNOS protein predominantly in the accumulating alveolar macrophages. OPN mRNA expression was also coinduced with iNOS mRNA, but was induced more slowly than iNOS mRNA in the lungs of ARDS mice. These results suggested that OPN, which may reduce NO production of macrophages by inhibiting iNOS expression, is significantly induced and expressed on alveolar macrophages in the lungs of ARDS. It is possible that OPN is partially involved in playing a protective role against excessive production of NO in ARDS.

Key words: Osteopontin—Macrophage—ARDS.

Correspondence to: Fumiyuki Takahashi; email: fumiyuki@med.juntendo.ac.jp

Introduction

Acute respiratory distress syndrome (ARDS) is characterized by an edematous reaction in the lung, leading to defective gas exchange, and carries a high mortality rate [1, 2]. ARDS frequently occurs following sepsis caused by gram-negative bacterial infection, aspiration of gastric contents, major trauma, or other clinical events [2]. Although many researchers have investigated the pathogenesis of ARDS, its cause remains largely unknown. Superoxide anion and proteolytic enzymes produced by activated neutrophils induce marked lung injury in ARDS [3–5]. Thus, the sequestration and subsequent activation of neutrophils in the lung are considered to be essential in the development of ARDS [1]. However, it has been demonstrated that neutrophil-depleted mice are still susceptible to lipopolysaccharide (LPS) in the development of ARDS [6].

Recent studies suggest that activated macrophages are also essential in the pathogenesis of ARDS. Stimulation of macrophages with LPS and various cytokines induces inducible nitric oxide synthase (iNOS) expression, resulting in elevated nitric oxide (NO) production [7]. The interaction of NO induced by iNOS with superoxide anion generated from macrophages or neutrophils forms a potent reactive oxidant, peroxynitrite, which induces severe tissue damage [8, 9]. It has therefore been suggested that increased output of NO production by alveolar macrophages stimulated with LPS is partially involved in mediating acute lung injury in ARDS. A number of studies support this hypothesis: Arkovits et al. [10] reported that selective iNOS inhibitors prevent pulmonary transvascular flux caused by LPS injection in a rat model Wu et al. [11] also demonstrated that the selective iNOS inhibitor aminoguanidine improves survival in an animal model for endotoxic shock induced by LPS. Similarly, lung damage after LPS injection is markedly reduced in iNOS-deficient mice compared with wild-type mice, as evaluated by the lung wet/dry ratio and lactate dehydrogenase content in BAL fluid [12]. These reports suggest that increased output of NO production mediated by iNOS from activated macrophages contributes to the development of acute lung injury/ARDS.

Osteopontin (OPN) is a secreted, arginine-glycine-aspartic acid (RGD)-containing phosphoglycoprotein with cell-adhesive and migratory properties [3, 14]. It has been demonstrated to be expressed in a variety of cells including cancer cells, osteoclasts, activated T cells, and activated macrophages [15–17]. Other than cell-adhesive and migratory functions, OPN has many other novel properties, suggesting that it may act as a cytokine and chemokine in various pathological conditions [18–20]. Recently, several investigators have demonstrated that OPN is capable of inhibiting NO production by suppressing iNOS expression in macrophages [21], renal epithelial cells [22], rat thoracic aorta [23], cardiac myocytes and microvascular endothelium [24]. It has been shown that endogenous OPN produced by activated macrophages inhibits cytotoxicity against tumor cells as a consequence of suppression of iNOS mRNA [21]. Scott et al. [23] reported that OPN suppresses iNOS activity in rat vascular tissues stimulated with LPS *in vitro*, suggesting that it may exert an anti-inflammatory effect during sepsis caused by gram-negative bacterial infection [23]. Singh et al. [24] demonstrated that glucocorticoids markedly